國立臺灣大學醫學院物理治療學系暨研究所

博士論文

School and Graduate Institute of Physical Therapy

College of Medicine

National Taiwan University

Doctoral Dissertation

應用影像學指標與足底壓力分析探討微創手術治療足部畸形之臨床與生物力學效應

Application of Imaging Parameters and Plantar Pressure Analysis for the Clinical and Biomechanical Effects of Minimally Invasive Surgery in Treating Foot Deformities

陳彥宇

Yanyu CHEN

指導教授：徐瑋勵 博士

Advisor: Wei-Li, Hsu, Ph.D.

中華民國 114 年 07 月

July 2025

doi:10.6342/NTU202501861

口試委員審定書

國立臺灣大學博士學位論文
口試委員會審定書

應用影像學指標與足底壓力分析探討微創手術治療足部畸形之臨床與生物力學效應

Application of Imaging Parameters and Plantar Pressure Analysis for the Clinical and Biomechanical Effects of Minimally Invasive Surgery in Treating Foot Deformities

本論文係陳彥宇君（學號 D02428002）在國立臺灣大學物理治療學系暨研究所完成之博士學位論文，於民國 114 年 6 月 21 日承下列考試委員審查通過及口試及格，特此證明

口試委員： 徐瑋勵 （簽名）

（指導教授）

王廷明　吳柏廷

王頎麟　蔡俊灝

系主任、所長 王淑芬 （簽名）

doi:10.6342/NTU202501861

ACKNOWLEDGEMENTS

First and foremost, I would like to express my deepest gratitude to my advisor, Professor Wei-Li Hsu, for her invaluable guidance and encouragement throughout my doctoral journey. Her expertise in biomechanics and her insightful advice were crucial to the completion of this research.

I am grateful to the faculty and staff of the School and Graduate Institute of Physical Therapy, National Taiwan University, for providing an excellent academic environment and the resources necessary for my work. I also wish to thank my colleagues at Show Chwan Memorial Hospital, especially the foot and ankle team, for their support in both clinical and research aspects.

I am indebted to all the patients who participated in the studies, as their willingness to contribute their data made this research possible. My thanks also go to the research assistants and study nurses who helped with data collection and analysis.

Finally, I would like to thank my family for their unconditional love and support. My wife and children have been my source of strength and motivation, and this achievement would not have been possible without their understanding and patience.

To all who have contributed to this work in ways both big and small, I offer my sincere thanks.

doi:10.6342/NTU202501861

中文摘要

足部畸形如扁平足（flatfoot）、拇趾外翻（hallux valgus, HV）及蹠骨內收（metatarsus adductus, MA）等，都是臨床上常見的足部問題，可能對患者的生活品質與行動能力造成顯著影響。微創手術在矯正足部畸形方面具有顯著優勢，相比傳統開放手術，微創手術不僅切口小、出血少、疼痛減輕，術後恢復快，而且對患者肢體的生物力學環境影響較小。

在臨床評估中，影像學指標和生物力學評估方法密不可分。影像學指標能夠清晰顯示骨骼結構和關節排列情況，是診斷和治療規劃的重要工具。生物力學評估，特別是足底壓力分析，則提供了動態的功能性數據，有助於了解手術對足部功能的影響。

本研究將結合影像學指標和足底壓力分析，全面探討微創手術治療足部畸形的臨床和生物力學效應，以期為臨床治療提供更為科學的評估和決策依據。具體的研究目的與結果如下：

目的一： 了解兒童扁平足接受微創矯正手術的術後長期結果與其影響因子。

doi:10.6342/NTU202501861

本研究回溯性納入自 2011 到 2015 年在彰化秀傳醫院接受距下關節限制術的扁平足患者，分析手術前後的影像學指標與足底壓力分佈（根據 Viladot 分類），再分析其與功能表現的相關性。

研究共納入了 19 位病患的 38 隻腳，接受手術時的平均年齡為 11±1.79 歲，平均追蹤時間為 10±1.4 年。手術後所有的足部影像學指標均有顯著的改善，而足底壓力分佈（根據 Viladot 分類）有 71%的足部分類為正常足型。功能表現依據 AOFAS-hindfoot score 和 FAOS score，有 82%的病患有 Good to excellent 的評分。而後根據 ROC curve 分析，手術前的 talonavicular coverage angle 小於 28.5 度、Meary's angle 小於 19.5 度、以及 talar declination angle 小於 37.5 度可以預測較佳的長期術後功能表現。

<u>目的二</u>：了解拇趾外翻微創矯正手術對前足壓力的影響與其原因。

本研究前瞻性納入中度到重度拇趾外翻並接受 MICA 手術之患者，記錄手術前與術後三個月的 X 光影像及動態足底壓力分析（Footscan®, RSscan International, Olen, Belgium），再分析影像學指標與足底壓力變化的相關性。

研究共納入了 25 位患者的 31 隻腳，平均年齡為 50.83±12.38 歲。手術前後與拇趾外翻相關的影像學指標均有顯著的改善；而第一蹠骨的長度在術後有統計學

doi:10.6342/NTU202501861

顯著地縮短了 2.3mm，雖然第二蹠骨的相對長度與側面的 Meary’s angle 並無統計學顯著的改變。足底壓力的部分，中央蹠骨區域的最大受力、最大壓力、累積受力、與累積壓力在手術前後都沒有統計學顯著的差異。反而是第一蹠骨與拇趾區域的壓力參數，在術後三個月有統計學顯著的降低。

目的三：了解拇趾外翻與蹠骨內收微創矯正手術對前足壓力的影響與其原因

研究前瞻性納入拇趾外翻併發蹠骨內收與蹠痛症（metatarsalgia）的患者，記錄手術前與術後六個月的 X 光影像及動態足底壓力分析，再分析術後 X 光影像學指標與足底壓力改變間的相關性。數據來自 2021 年 8 月至 2023 年 7 月期間由單一醫師治療的 25 名患者（25 隻腳），平均年齡為 50.1 歲。影像學分析顯示，術後六個月 HVA、IMA 及 MA 均有顯著改善。而足底壓力評估顯示，術後六個月，第 2 至第 4 蹠骨區域的最大受力、峰值壓力、受力時間積分及壓力時間積分均顯著降低。

實驗設計：回溯性研究，前瞻式介入研究

關鍵字：扁平足、距下關節限制術、拇趾外翻、蹠骨內收、微創手術、足底壓力

doi:10.6342/NTU202501861

ABSTRACT

Deformities of the foot such as flatfoot, hallux valgus (HV), and metatarsus adductus (MA) are common clinical foot problems that can significantly impact the quality of life and mobility of patients. Minimally invasive surgery (MIS) has significant advantages in correcting foot deformities. Compared to traditional open surgery, MIS offers smaller incisions, less bleeding, reduced pain, and faster recovery. It also causes less damage to surrounding muscles and other soft tissues, thereby having a smaller impact on the biomechanical environment of the limb.

In clinical evaluations, imaging indicators and biomechanical assessment methods are closely related. Imaging indicators such as X-rays, CT scans, and MRI can clearly show the structure of bones and the alignment of joints, serving as important tools for diagnosis and treatment planning. Biomechanical assessment, especially plantar pressure analysis, an accurately measure the pressure distribution in different areas of the foot, reflecting changes in gait and weight-bearing conditions and providing important evidence for postoperative outcome evaluation.

This study will combine imaging indicators and plantar pressure analysis to comprehensively explore the clinical and biomechanical effects of minimally invasive surgery for treating foot deformities, aiming to provide more scientific evaluation and decision-making basis for clinical treatment. The specific research aims are as follows:

Aim 1: **The aim 1 is to understand the long-term results of pediatric flat foot receiving minimally invasive correction and to determine the predictive factors.**

Conducted as a retrospective analysis, it included patients who underwent the procedure at Show-Chwan Memorial Hospital between 2011 and 2015. Correlations

doi:10.6342/NTU202501861

between radiographic measurements and plantar pressure distribution, as classified by the Viladot system, were also examined.

A total of 19 patients (38 feet) participated in the study, with an average age of 11 ± 1.79 years at the time of surgery and a mean follow-up period of 10 ± 1.4 years. Postoperative radiographic parameters demonstrated significant improvements across all cases. Additionally, plantar pressure distribution analysis classified 71% of feet as having a normal foot type based on the Viladot classification. Functional outcomes, evaluated through the AOFAS hindfoot scale and FAOS, showed that 82% of participants achieved good to excellent results. Moreover, ROC curve analysis identified preoperative talonavicular coverage angles of less than 28.5°, Meary's angles below 19.5°, and talar declination angles under 37.5° as predictors of more favorable long-term functional outcomes.

Aim 2: The aim 2 is to understand the pedobarographic results of minimally invasive hallux valgus correction surgery and to determine its reasons.

The research prospectively enrolled patients with moderate to severe hallux valgus treated with MICA. Radiographic data and dynamic plantar pressure measurements (Footscan®, RSscan International, Olen, Belgium) were collected preoperatively and three months postoperatively to explore correlations between imaging and pedobarographic parameters.

A total of 25 patients (31 feet) were included, with a mean age of 50.83 ± 12.38 years. Radiographic parameters associated with hallux valgus, including HVA, IMA, DMAA, 1MTLHS, and LSG, showed statistically significant postoperative improvement. Additionally, the first metatarsal length was reduced by 2.3 mm following surgery. However, no significant changes were observed in the relative length of the second metatarsal or the lateral Meary's angle. Regarding plantar pressure, central metatarsal

doi:10.6342/NTU202501861

regions showed no significant differences in maximum force, peak pressure, cumulative force, or cumulative pressure pre- and post-surgery. In contrast, pressure parameters in the first metatarsal and hallux regions demonstrated a significant decrease three months after surgery.

<u>Aim 3:</u> **The aim 3 is to understand the pedobarographic results of combined minimally invasive correction of hallux valgus and central metatarsals and to determine its reasons.**

This study prospectively included patients with hallux valgus, metatarsus adductus, and metatarsalgia, recording X-ray images and dynamic plantar pressure analysis (Footscan®, RSscan International, Olen, Belgium) preoperatively and six months postoperatively. The correlation between radiographic and pedobarographic parameters was then analyzed. Data were collected from 25 patients (25 feet) treated by a single surgeon between August 2021 and July 2023, with an average age of 50.1 years. Radiographic analysis revealed significant postoperative improvements in the hallux valgus angle (HVA), intermetatarsal angle (IMA), and metatarsus adductus angle (MA) six months after surgery. Pedobarographic evaluation showed reduced maximum force, peak pressure, force-time integral, and pressure-time integral in the second to fourth metatarsal regions six months after surgery.

Study Design: Retrospective cohort study, prospective cohort study.

Keywords: flatfoot, subtalar arthroereisis, hallux valgus, metatarsus adductus, minimally invasive surgery, plantar pressure.

doi:10.6342/NTU202501861

CONTENTS

doi:10.6342/NTU202501861

doi:10.6342/NTU202501861

doi:10.6342/NTU202501861

doi:10.6342/NTU202501861

CHAPTER 1 INTRODUCTION

Foot deformities such as flexible flatfoot (FFF), hallux valgus (HV), and metatarsus adductus (MA) significantly impact patients' mobility and quality of life, often necessitating surgical intervention when conservative treatments fail. With the advance in minimally invasive surgery, the postoperative pain, length of hospital stay, perioperative complications, and patients' satisfaction improved significantly. However, there are scarce evidence of long-term re sults in pediatric flexible flat foot receiving surgery, biomechanical impacts of forefoot deformities after percutaneous correction, and factors affecting these clinical outcomes. As the result, three aims are developed in the current study to fill this knowledge gap.

1.1 Flexible Flatfoot and Subtalar Arthroereisis

Flexible flatfoot (FFF), also referred to as pes planus, is a prevalent orthopedic condition among children, often presenting without symptoms.[1] Treatment becomes necessary in cases where patients experience fatigue, abnormalities in gait, or pain. Non-invasive approaches, such as the use of orthotics and stretching exercises targeting the Achilles tendon, generally yield positive results for managing FFF.[1, 2] However, when conservative strategies fail to resolve the deformity, surgical options like subtalar arthroereisis (STA), osteotomies, or tendon lengthening and transfers are considered.[2]

STA is a procedure that involves inserting an implant into the sinus tarsi to limit excessive eversion of the subtalar joint. Due to its minimally invasive approach, STA has gained popularity as an effective method for addressing flatfoot deformities.[3-5] This technique offers several advantages, including three-dimensional correction, minimal surgical trauma, and faster recovery times postoperatively.[6, 7] Nonetheless,

doi:10.6342/NTU202501861

most available data focus on short- to mid-term outcomes derived from retrospective analyses. To date, only one study has provided evidence of satisfactory long-term outcomes, spanning 15 years, for patients treated with bioabsorbable STA implants.[8] The primary objective of this study is to evaluate the long-term effectiveness of minimally invasive correction in pediatric flatfoot and to identify factors predictive of successful outcomes.

1.2 Hallux Valgus and Pedobarographic Analysis

Hallux valgus (HV) deformity contributes to both structural and functional impairments of the affected foot.[9]. Structural changes are well-documented using weight-bearing radiographs, which remain a fundamental tool for assessing HV deformity.[9]. Equally important but more challenging is the evaluation of functional impairments. While clinical indicators such as plantar callosities[10], and assessment tools like the American Orthopaedic Foot & Ankle Society (AOFAS) score[11] and the Manchester-Oxford Foot Questionnaire (MOXFQ)[12] provide insight into functional status, pedobarographic analysis offers an objective and quantitative method for examining foot biomechanics and functionality.[13-15].

However, there is no clear consensus regarding pedobarographic alterations in HV-affected feet. Studies have reported varying findings: Bryant et al.[16] observed increased loading on the hallux and first metatarsal head, Hida et al.[17] noted reduced hallux loading, and Hofmann et al.[18] identified increased pressure on the fourth and fifth toes in HV patients. These discrepancies may stem from differences in study populations, as HV encompasses a wide range of severity and associated conditions.[9]. Additionally, the variability in control group selection likely contributes to inconsistent results.[17, 19].

doi:10.6342/NTU202501861

Despite these variations, there is general agreement that central metatarsal loading tends to be elevated in HV patients.

Pedobarographic changes following HV correction have also been studied in various surgical techniques, including distal metatarsal osteotomy[20-26], proximal metatarsal osteotomy[27], and first tarsometatarsal joints fusion.[25, 28] However, the results from these studies remain diverse and inconclusive for different foot regions. The minimally invasive Chevron-Akin (MICA) osteotomy has shown promising radiographic and clinical outcomes for HV correction,[11, 12, 29-32] yet, to date, no research has investigated the pedobarographic changes associated with this procedure.

Metatarsalgia, a symptom frequently linked to HV, may indicate underlying pedobarographic abnormalities[33] and often necessitates additional procedures on the lesser toes.[34]. The term "transfer metatarsalgia" suggests that hallux valgus deformity may contribute to this condition and that correcting HV could potentially resolve it. However, existing literature does not clearly establish whether correcting HV alone is sufficient to address "transfer metatarsalgia." Therefore, the second aim of this study is to analyze the pedobarographic outcomes of minimally invasive HV correction surgery and to identify the factors contributing to these changes.

1.3 Hallux Valgus and Metatarsus Adductus

The development of Metatarsus Adductus (MA) may be associated with abnormal fetal foot positioning, although the exact cause remains unclear. Notably, approximately 30% of individuals with HV also present with MA, which can complicate surgical intervention and increase the recurrence rate of HV[35].

Previous research by Larholt and Kilmartin[36] examined 27 patients with both HV and MA who underwent rotation scarf and Akin osteotomy without lesser metatarsal

doi:10.6342/NTU202501861

surgery. Postoperatively, the Hallux Valgus Angle (HVA) improved from 34.6° to 13.2°. However, 42% of patients still had an HVA greater than 15° at the final follow-up. The authors suggested that the presence of MA could result in a residual valgus angle at the Metatarsophalangeal (MTP) joint, leading to less correction of the HVA.

Sharma et al[37] proposed a surgical algorithm for severe HV with MA, which included the Lapidus procedure, Akin closing wedge osteotomy, Weil's osteotomy, proximal oblique rotational metatarsal osteotomy, and medial sliding calcaneal osteotomy. Postoperative care involved six weeks of non-weight bearing. To expedite recovery and minimize soft tissue trauma, some surgeons have begun performing the Minimally Invasive Chevron Akin procedure (MICA) in conjunction with either Proximal[38] or Distal[39] Minimally Invasive Metatarsal Osteotomy. This approach allows patients to bear weight immediately postoperatively, with less associated soft tissue trauma.

Previous studies have demonstrated a significant lateral shift in load distribution in feet with HV[40, 41]. Furthermore, MA has been associated with increased peak pressure and impulse over the heel, lateral midfoot, and lateral forefoot compared to normal feet[42]. Despite these findings, there is a paucity of research examining pedograph changes following hallux valgus surgery with metatarsal osteotomy. Hence, the Aim 3 of this study is to understand the pedobarographic results of combined minimally invasive correction of hallux valgus and central metatarsals and to determine its reasons.

As a foot and ankle surgeon with more than ten years of experience in minimally invasive techniques, and also as a doctoral student in physical therapy, I have always been interested in how surgery changes foot function from a biomechanical point of view. Many patients choose minimally invasive surgery (MIS) because it offers smaller wounds, faster recovery, and less soft tissue damage. However, we still do not fully understand

doi:10.6342/NTU202501861

how these surgical methods affect foot pressure during walking or how they influence long-term function.

This dissertation brings together my clinical experience and research training. It focuses on three common foot deformities: flatfoot, hallux valgus, and metatarsus adductus. These studies use both imaging and plantar pressure analysis to better understand how MIS changes the alignment and loading of the foot. By combining surgical results with biomechanical data, I hope this work will help improve how we plan surgeries and guide physical therapy before and after operations.

doi:10.6342/NTU202501861

CHAPTER 2 Study One: Subtalar Arthroereisis for Pediatric Flexible Flat Foot

(This study has been published.[43])

2.1 Research questions

2.1.1) What is the long-term radiographic, pedobarographic, and clinical outcomes of pediatric FFF underwent STA?

2.1.2) Is there any perioperative radiographic or pedobarographic parameter that can predict the postoperative functional outcome of pediatric FF underwent STA?

2.1.3) If there is predictive factor for postoperative functional outcome, what is the cut-off value of these parameters to predict better clinical result?

2.2 Study purposes

2.2.1) To report the long-term radiographic, pedobarographic, and clinical outcomes of pediatric FFF underwent STA in a single institute.

2.2.2) To explore the correlation of perioperative radiographic and pedobarographic parameters to postoperative functional outcome of pediatric FFF underwent STA.

2.2.3) To determine the cut-off value of parameters identified to predict better clinical result.

2.3 Hypothesis

The null hypotheses of this study are:

doi:10.6342/NTU202501861

2.3.1) The perioperative radiographic and pedobarographic parameters are not statistically significantly correlated with the postoperative functional outcomes in pediatric flexible flatfoot patients who underwent subtalar arthroereisis (STA).

2.4 Study design (Figure 1)

This study was conducted as a single-center, retrospective cohort analysis. Following approval from the Institutional Review Board of Show-Chwan Memorial Hospital (SCMH_IRB-1110703; see Appendix 1), electronic medical records were reviewed. The study adhered to the principles outlined in the Declaration of Helsinki and complied with the Health Insurance Portability and Accountability Act (HIPAA).

2.5 Participants

From 2011 to 2015, a total of 68 potential candidates who had received STA for the treatment of symptomatic FFF were identified.

2.5.1) Inclusion criteria

Patients aged between 9 and 13 years old, received STA in Show-Chwan Memorial Hospital under the diagnosis of FFF.

2.5.2) Exclusion criteria

Patients were excluded if they had rigid flatfoot, residual deformities from clubfoot, a history of previous lower limb trauma or surgical interventions, neurogenic or neuromuscular conditions, generalized joint hypermobility, or if they had undergone procedures beyond Achilles tendon lengthening or accessory navicular removal. Additionally, individuals with incomplete radiographic assessments were also excluded.

doi:10.6342/NTU202501861

2.6 Surgical procedures of subtalar arthroereisis (STA)

2.6.1) Prosthesis

This study employed two different types of implants: the titanium alloy Talar-Fit (Osteomed, Addison, TX, USA) and the polyethylene disk-and-peg implant (STA-Peg, Wright Medical). The Talar-Fit implant has a cone-shaped design specifically crafted to align with the anatomical structure of the sinus tarsi. It features a hollow center to facilitate precise placement and incorporates deep threads to promote tissue integration and enhance stability. Conversely, the STA-Peg is positioned on the dorsal aspect of the calcaneus, just anterior to the posterior facet, and is secured using a stem inserted into a predrilled hole in the calcaneus. Both implants are designed to limit excessive eversion of the talus, correct valgus deformity of the heel, and reestablish the medial longitudinal arch.

2.6.2) Surgical techniques for Talar-fit (Figure 2)

An incision was made approximately 1 cm anterior and 1 cm inferior to the lateral malleolus. The tarsal sinus was exposed using blunt dissection. A guide pin was inserted into the sinus tarsi and carefully advanced through the tarsal canal. Sequential implant trials were performed while maintaining the subtalar joint in an inverted position. Once the appropriate implant size was identified, the trial implant was removed, and the final implant was inserted. The position of the implant and the range of motion (ROM) of the subtalar joint were confirmed using fluoroscopic imaging. The surgical site was then irrigated, closed in layers, and dressed with a compression dressing.

doi:10.6342/NTU202501861

2.6.3) Surgical techniques for STA-Peg

A curved incision was made along the sinus tarsi, and blunt dissection was performed to expose the tarsal sinus. The foot was positioned in supination to allow clear visualization of the posterior articular facet of the calcaneus. Using a guide and drill specific to the STA-Peg system, a hole was prepared anterior to the posterior facet of the calcaneus. Sizing trials were conducted to determine the most appropriate implant size, after which the STA-Peg implant was securely cemented in place. The implant's positioning and the range of motion (ROM) of the subtalar joint were assessed under fluoroscopic guidance. The surgical site was thoroughly irrigated, closed in layers, and dressed with a compression bandage.

2.6.4) Postoperative Protocol

To stabilize the ankle joint in a neutral position, a short leg splint was applied for the first four weeks after surgery. Gradual weight-bearing was permitted as tolerated immediately following the procedure. Follow-up visits were scheduled at 2, 4, and 8 weeks postoperatively in the outpatient clinic.

2.7 Data Collection

2.7.1) Demographic Data

Age when they received surgery, gender, laterality of the feet operated, and type of prosthesis used were collected and recorded.

2.7.2) Radiographic Parameters (Figure 3)

Radiographs of the operated foot, including preoperative and immediate postoperative standard weight-bearing anteroposterior and lateral views, were accessed from the digital

doi:10.6342/NTU202501861

database. Additional weight-bearing radiographs in anteroposterior and lateral projections were acquired during the final outpatient follow-up visit. Key measurements taken from the anteroposterior radiographs included the talonavicular coverage angle, talar–first metatarsal angle, Kite's angle (anteroposterior talocalcaneal angle), and the fibular axis calcaneal offset (FACO). From the lateral radiographs, parameters such as Meary's angle (lateral talar–first metatarsal angle), calcaneal inclination, talar declination, talocalcaneal angle, and the Moreau-Costa-Bartani angle were analyzed. A detailed explanation of these radiographic metrics is presented in Table 1.

2.7.3) Pedobarographic outcome, functional performance and patient-reported outcomes

Pedobarographic, functional, and patient-reported outcomes were evaluated exclusively during the final follow-up period.

Pedobarographic data were obtained using a podoscope, with the degree of plantar arch collapse categorized based on Viladot's classification system, which ranges from grades 0 to 4.

Functional performance was assessed using the American Orthopaedic Foot & Ankle Society (AOFAS) ankle-hindfoot scale during the last outpatient visit. The AOFAS scale evaluates three key aspects: pain, function, and alignment, with a total possible score of 100. Scores were classified into the following categories: excellent (85-100), good (75-84), fair (65-74), and poor (below 65).

Patient-reported outcomes were measured using the Foot and Ankle Outcome Score (FAOS) during the same outpatient visit. The FAOS has a maximum score of 100 and was categorized as follows: excellent (90-100), good (80-89), fair (70-79), and poor (below 70).

doi:10.6342/NTU202501861

2.8 Statistical Analysis

Radiographic angles, along with AOFAS ankle-hindfoot and FAOS scores, were presented as mean values accompanied by their respective standard deviations (SD).

2.8.1) Perioperative comparison

Radiographic angles recorded before and after surgery were evaluated using the paired Student's t-test. Additionally, subgroup analyses were performed to compare radiographic and functional outcomes between male and female patients.

2.8.2) Factors that may affect long-term functional outcomes

To examine the relationship between different factors and long-term functional outcomes, Pearson correlation coefficients were calculated. Factors assessed included the age at the time of surgery, preoperative and postoperative radiographic measurements, as well as the changes in radiographic angles observed between the two time points.

2.8.3) Cut-off value analysis

To identify optimal cutoff values for predicting favorable clinical outcomes, ROC (receiver operating characteristic) curves were created for the radiographic factors that showed statistical significance in the previous analysis. Favorable outcomes were defined as an AOFAS score greater than 85 and a FAOS score exceeding 80. The area under the curve (AUC) was determined for each radiographic parameter. The Youden index, calculated as (sensitivity + specificity − 1), was utilized to pinpoint the ideal cutoff values. These thresholds were then used to calculate the positive and negative predictive values associated with the diagnostic tests.

doi:10.6342/NTU202501861

2.8.4) Statistical analysis software

Statistical analyses were performed using SPSS software, version 23.0 (IBM, Armonk, NY, USA). A p-value of less than 0.05 was considered to indicate statistical significance.

2.9 Results

2.9.1) General Demographics

Initially, 68 potential participants were identified for this study. Four individuals were excluded due to missing medical records, and eight were excluded as they exceeded the age limit of 13 years. Of the remaining participants, 25 (45%) were female, and 31 (55%) were male. The average age at the time of surgery was 11.3 years, ranging from 9 to 13 years. Bilateral foot involvement was present in 52 (92%) patients. Among them, 45 (80%) received Talar-Fit implants, while 11 (20%) underwent STA-Peg implantation. Implant removal was necessary for four feet due to irritation and for another four feet due to implant dislodgement.

From these, 19 patients (38 feet) were included in our analysis. This group consisted of 10 females (52%) and 9 males (48%), with an average age of 11 years at surgery (range: 9–13 years). All underwent bilateral STA procedures, with 16 feet (84%) receiving Talar-Fit implants and 3 feet (16%) receiving STA-Peg implants. The average follow-up duration was 10 years, ranging from 9 to 13 years. Importantly, none of the patients in this cohort underwent any additional procedures alongside STA.

2.9.2) Radiographic Outcomes

Analysis of radiographic outcomes based on standard weight-bearing anteroposterior radiographs revealed significant reductions in several key angles. The talonavicular

doi:10.6342/NTU202501861

coverage angle decreased by an average of 16° ($p < 0.001$), while the anteroposterior talar–first metatarsal angle showed a mean reduction of 9.6° ($p < 0.001$). Similarly, the lateral talar–first metatarsal angle decreased by 8.6° on average ($p < 0.001$).

On lateral weight-bearing radiographs, notable decreases were observed in the talar–first metatarsal angle (mean reduction of 10.0°, $p < 0.001$), talar declination angle (mean reduction of 7.6°, $p < 0.001$), lateral talocalcaneal angle (mean reduction of 4.1°, $p < 0.001$), and Moreau-Costa-Bartani angle (mean reduction of 12.9°, $p < 0.001$). Additionally, the fibular axis calcaneal offset (FACO) decreased by an average of 3.1° ($p < 0.001$). In contrast, the calcaneal inclination angle demonstrated a significant mean increase of 3.7° ($p < 0.001$).

2.9.3) Functional and patient-reported outcomes

Using the Viladot classification system, 27 feet were identified as normal, 9 as grade I, and 2 as grade II. At the final follow-up, the mean AOFAS score was 88.6, with a range of 54 to 100. Patient outcomes were categorized as excellent in 15 cases, good in 1 case, fair in 2 cases, and poor in 1 case. Similarly, the mean FAOS at the final follow-up was 91.3, with scores ranging from 72 to 100. Among these, 12 patients were rated as excellent, 4 as good, and 3 as fair. Overall, 84.2% of the participants achieved good to excellent functional outcomes as reflected by both the AOFAS and FAOS scoring systems.

2.9.4) Subgroup analysis

A comparison between male and female groups revealed no statistically significant differences in the changes in angles from preoperative to postoperative measurements. Male patients had slightly higher AOFAS scores (94.2) compared to female patients (83.7), with a p-value of 0.06. Similarly, FAOS scores were marginally higher in male

doi:10.6342/NTU202501861

patients (94.8) than in female patients (87.7), although this difference was not statistically significant ($p = 0.08$).

2.9.5) Correlation analysis

The correlations between the evaluated variables and functional outcomes are outlined in Table 2. No significant association was found between patient age and either the AOFAS or FAOS scores.

Preoperative radiographic measurements showed several notable correlations with functional outcomes. The AOFAS score was significantly associated with the talonavicular coverage angle ($r = -0.70$, $p < 0.01$), anteroposterior talocalcaneal angle ($r = -0.39$, $p = 0.01$), lateral talar–first metatarsal angle ($r = -0.65$, $p < 0.01$), talar declination angle ($r = -0.40$, $p = 0.01$), calcaneal inclination angle ($r = 0.35$, $p = 0.03$), and lateral talocalcaneal angle ($r = 0.38$, $p = 0.02$). Similarly, significant correlations were found between the FAOS score and the talonavicular coverage angle ($r = -0.50$, $p < 0.01$), lateral talar–first metatarsal angle ($r = -0.48$, $p < 0.01$), talar declination angle ($r = -0.44$, $p < 0.01$), and lateral talocalcaneal angle ($r = -0.44$, $p < 0.01$).

Postoperative radiographic measurements also revealed significant relationships with functional outcomes. The AOFAS score was correlated with the talonavicular coverage angle ($r = -0.65$, $p < 0.01$), lateral talar–first metatarsal angle ($r = -0.51$, $p < 0.01$), and talar declination angle ($r = -0.49$, $p < 0.01$). The FAOS score also demonstrated significant correlations with the talonavicular coverage angle ($r = -0.50$, $p < 0.01$), anteroposterior talocalcaneal angle ($r = -0.47$, $p < 0.01$), lateral talar–first metatarsal angle ($r = -0.57$, $p < 0.01$), talar declination angle ($r = -0.63$, $p < 0.01$), and lateral talocalcaneal angle ($r = -0.36$, $p = 0.02$).

doi:10.6342/NTU202501861

When examining the changes in angles between preoperative and postoperative measurements, the lateral talar–first metatarsal angle change ($r = -0.44$, $p < 0.01$) and calcaneal inclination change ($r = 0.37$, $p = 0.02$) were significantly correlated with the AOFAS score. However, no significant relationship was observed between angle changes and the FAOS score.

2.9.6) ROC curve

The information presented in Table 3, generated through ROC curve analysis, differentiates between "Excellent" and "Inferior Outcomes" for AOFAS scores and "Good to Excellent" and "Inferior Outcomes" for FAOS scores. Interestingly, the cutoff values for talonavicular coverage, Meary’s angle, and talar declination were consistent across both scoring systems, measured at 28.5°, 19.5°, and 37.5°, respectively.

For the AOFAS score, the calculated area under the curve (AUC) values were 0.74 (95% CI: 0.63–0.85) for talonavicular coverage, 0.70 (95% CI: 0.56–0.84) for Meary’s angle, and 0.70 (95% CI: 0.61–0.79) for talar declination. For the FAOS score, the AUC values were 0.90 (95% CI: 0.86–0.94) for talonavicular coverage, 0.93 (95% CI: 0.89–0.97) for Meary’s angle, and 0.77 (95% CI: 0.68–0.86) for talar declination.

Effect size and post-hoc power calculations were performed to determine whether the sample size was sufficient. Based on the AOFAS and FAOS scales, patient-acceptable symptomatic status was achieved by 30 out of 38 and 32 out of 38 patients, respectively, with corresponding odds ratios of 3.54 and 4.88. Post-hoc power values were calculated as 0.94 for the AOFAS scale and 0.98 for the FAOS scale, confirming that the sample size was adequate for the study.

doi:10.6342/NTU202501861

2.9.7) Complications

During the final follow-up, six feet were reported to experience sinus tarsi pain. Despite this, none of the affected patients chose to have their implants removed. As a result, unlike findings reported in some previous studies, no implant removals were performed in our cohort throughout the follow-up period.

2.10 Discussion

The role of subtalar arthroereisis (STA) in treating flexible flatfoot (FFF) in children remains a topic of debate, primarily due to the limited availability of long-term data on its effectiveness and potential complications.[3, 4, 44] This study aimed to evaluate the long-term outcomes of using non-absorbable endo-orthosis for pediatric FFF and to identify predictive factors for improved results. Our findings suggest that STA significantly enhances deformity correction, as evidenced by radiographic parameters, and contributes to improved functional performance, as reflected in AOFAS and FAOS scores. Additionally, preoperative thresholds were established to guide surgical decision-making and optimize patient outcomes.

Radiographic assessments revealed substantial improvements across all parameters following STA. Similar findings have been reported in prior short- and mid-term follow-ups.[45-48] For instance, Indino et al. examined 56 patients (112 feet) and found that deformity corrections achieved with STA were maintained into skeletal maturity. Their analysis focused on parameters such as the talonavicular angle, uncoverage percentage, lateral talocalcaneal angle, calcaneal pitch, and Meary's angle.[45] Another study by Mazzotti et al. showed significant radiographic improvements over an average follow-up of 15 years using bioabsorbable implants for FFF treatment.[8] Our results

doi:10.6342/NTU202501861

align with these studies, further supporting the long-term effectiveness of STA in maintaining deformity correction.

The Viladot classification system, recognized for its strong reliability, is a widely used tool for evaluating the severity of medial longitudinal arch collapse.[49] In Mazzotti's research, 73.4% of patients achieved a physiologic footprint (Viladot grade 0), and 20.3% were classified as grade I at the final follow-up.[8] Similarly, in this study, 71% of cases were graded as Viladot grade 0, and 23% as grade I, indicating that STA effectively restores the medial arch in pediatric FFF cases.

Clinically, 84% of patients reported good to excellent outcomes based on AOFAS and FAOS scores, consistent with findings in the literature. A review by Tan et al. reported an 88% rate of good to excellent outcomes for STA.[6] Similarly, Mazzotti et al. observed that 88.2% of patients were satisfied with their results, noting significant improvements in pain and functional ability.[8] Our study highlights that lower preoperative and postoperative values for talonavicular coverage, Meary's angle, and talar declination are key predictors of favorable outcomes.

Complications such as chronic sinus tarsi pain, implant migration, and peroneal muscle contracture are commonly reported following STA. In this study, sinus tarsi pain was observed in 15% of cases, consistent with the 10-40% range cited in previous studies.[27, 48, 50-52] However, the underlying causes remain unclear. Cook et al. found no significant associations between sinus tarsi pain and variables such as patient age, gender, implant size, or the use of adjunctive procedures.[53]

Biomechanical studies, such as those by Prachgosin et al., emphasize functional impairments in untreated flatfoot, including medial arch deformation and abnormal ground reaction forces during gait.[54] Our findings reinforce the importance of

doi:10.6342/NTU202501861

addressing medial arch collapse and suggest using preoperative thresholds as a predictive tool. ROC curve analysis identified cutoff values of 28.5° for talonavicular coverage, 19.5° for Meary's angle, and 37.5° for talar declination, which can aid in assessing the suitability of STA and setting realistic expectations for patients.

Several limitations of this study must be acknowledged. The retrospective design and single-institution setting may introduce selection bias and limit generalizability, particularly given the small sample size. The relatively high attrition observed in this study is largely attributable to the participants' life transitions. By the time of the final follow-up, most of the children had reached adulthood and had relocated—often to other cities or even abroad—for higher education or employment. Consequently, they were unable to return to the original institution for re-evaluation. This underscores the inherent challenge of conducting longitudinal studies that span childhood into adulthood, where geographic mobility significantly hampers long-term follow-up.

Furthermore, this study did not compare STA with alternative surgical techniques, such as osteotomies or tendon transfers. The use of two different implant types (Talar-Fit and STA-Peg), based on surgeon preference, may have influenced outcomes. Although no significant differences were noted between implant groups, the discontinuation of the STA-Peg during the study period resulted in fewer cases for this type. Additionally, implant size was not accounted for in this analysis. Future research involving larger, prospective studies is needed to further validate these findings and address these limitations.

doi:10.6342/NTU202501861

2.11 Conclusion

To conclude, our study demonstrates that STA represents an effective strategy for achieving sustained deformity correction and improved functional performance in managing FFF in pediatric patients. Patient-reported outcomes indicated that 84.2% of cases achieved good to excellent results, reflecting long-term functional enhancement and satisfaction. Both preoperative and postoperative radiographic angles emerged as significant predictors of functional outcomes. The identified preoperative threshold values offer critical insights to help guide the selection of suitable surgical candidates. The restoration of the medial longitudinal arch, coupled with the correction of forefoot abduction, proved to be essential elements in achieving successful deformity correction and enhanced functional results.

doi:10.6342/NTU202501861

CHAPTER 3 Study Two: Pedobarographic Analysis of Hallux Valgus Surgery

(This study has been published.[55])

3.1 Research questions

3.1.1) What is the pedobarographic change of 1st and central metatarsal after surgical correction of HV using MICA?

3.1.2) Do the perioperative pedobarographic changes correlate with radiographic changes?

3.2 Study purposes

3.2.1) To report the radiographic and plantar pressure changes of HV correction using MICA.

3.2.2) To explore the perioperative radiographic changes and discuss their potential effects on plantar pressure changes of HV correction using MICA.

3.3 Hypothesis

The null hypotheses of this study are:

3.3.1) There is no statistically significant changes in plantar pressure after HV correction using MICA.

3.4 Study design (Figure 4)

This research follows a single-center, prospective cross-sectional design and received approval from the Institutional Review Board of Changhua Show-Chwan Memorial Hospital (SCMH_IRB-1130409, refer to Appendix 2). The study was carried out in

doi:10.6342/NTU202501861

adherence to the principles outlined in the Declaration of Helsinki and in compliance with the Health Insurance Portability and Accountability Act.

3.5 Participants

All patients satisfying the specified inclusion and exclusion criteria underwent fourth-generation MICA[56] without any additional procedures involving the lesser toes. These patients were then included for subsequent follow-up and evaluation.

3.5.1) Inclusion criteria

Eligible patients included those aged 18 years or older, presenting with moderate to severe hallux valgus (HV), defined as an HV angle exceeding 20° or an intermetatarsal angle greater than 13°.[57, 58] These patients required surgical correction and reported symptoms confined to the hallux, with no associated involvement of the lesser metatarsals or toes.

3.5.2) Exclusion criteria

Exclusion criteria included patients presenting with metatarsalgia or plantar keratoses, those with other ipsilateral foot conditions apart from HV—such as metatarsus adductus, pes planus, or lesser toe deformities—individuals with a history of prior lower limb surgeries, those diagnosed with rheumatic diseases, or cases with incomplete data records.

3.6 Surgical techniques and postoperative protocols

3.6.1) Minimally Invasive Chevron Akin (MICA)

Patients with HV who did not exhibit first ray hypermobility and had not responded to conservative treatments were treated using fourth-generation Minimally Invasive

doi:10.6342/NTU202501861

Chevron Akin (MICA) osteotomy[59]. For patients without metatarsalgia or plantar keratoses, isolated MICA was performed. Conversely, those with these conditions underwent MICA combined with a lesser metatarsal shortening osteotomy. Anesthesia, tailored to surgical requirements, was provided as either general or spinal, and prophylactic antibiotics were administered in alignment with local medical protocols.

Patients were placed in a supine position with their feet extended beyond the edge of the operating table. Intraoperative fluoroscopic guidance was provided using a mini C-arm positioned on the side of the surgical site. The Chevron osteotomy was carried out at the distal metaphyseal-diaphyseal junction with a Shannon burr. A 3 mm Kirschner wire was retrogradely inserted from the osteotomy site into the diaphysis of the first metatarsal to aid in the correction and stabilization of the HV deformity. The osteotomy was then secured using two antegrade headless compression screws, which engaged both cortices. The bunion prominence and any excess bone on the proximal fragment were removed using the burr. Subsequently, an Akin osteotomy was performed on all patients, stabilized with a retrograde headless compression screw. Soft tissue procedures, such as abductor tenotomy, were not performed in this cohort. (Figure 5)

3.6.2) Postoperative protocol

Following the procedure, patients were provided with a soft hallux valgus splint (Bunion Adjustable Splint, DARCO Co.) and instructed to wear stiff-soled orthopedic footwear for a duration of six weeks. After this period, they were allowed to transition to wearing their choice of comfortable shoes without any restrictions. Full weight-bearing was encouraged immediately post-surgery.

doi:10.6342/NTU202501861

3.7 Data Collection

3.7.1) Radiographic parameters

To evaluate the surgical outcomes, weight-bearing radiographs were acquired preoperatively and three months after surgery. Key hallux valgus parameters, including the hallux valgus angle (HVA), intermetatarsal angle (IMA), and distal metatarsal articular angle (DMAA), were measured[58]. Additionally, the morphology of the lateral head of the first metatarsal (MT1LHS) [60, 61] and the grade of lateral sesamoid positioning (LSG)[62] were assessed to analyze rotational deformities of the first ray. The first metatarsal length (MT1L) and second metatarsal protrusion distance (MT2PD) [63] were recorded to investigate potential correlations with changes in metatarsal loading. To evaluate overall foot shape, lateral Meary's angle (LMA) and calcaneal pitch angle (CPA) were measured, and dorsiflexion malunion was noted as a potential complication.

Since no surgical alterations were made to the second metatarsals, their lengths on preoperative and postoperative dorsoplantar radiographs were assumed to remain unchanged. To adjust for magnification differences, the postoperative corrected length of the first metatarsal (MT1CL) was calculated using the second metatarsal length as a reference.

3.7.2) Pedobarographic parameters

In the testing environment, a pressure-measuring mat (dimensions: 325 mm by 488 mm, containing 4096 resistive sensors with a sampling frequency of 200 Hz; RSscan® International, Paal, Belgium) was embedded into a walking platform. To ensure precise foot placement on the sensor area, a two-step gait initiation protocol[64] was implemented. Patients were guided by a qualified physical therapist to familiarize

doi:10.6342/NTU202501861

themselves with the walkway, practicing barefoot several times to achieve a consistent and natural walking rhythm.

This protocol was conducted both preoperatively and at three months postoperatively. Each participant completed a minimum of three walking trials along the track. Before initiating data collection, the patients' body weight and shoe size were calibrated within the system. Dynamic plantar pressure measurements were recorded using Footscan® 7 Gait 2nd Generation software (RSscan International, Olen, Belgium), which automatically divided each foot into ten anatomical regions: hallux, lesser toes, metatarsals one to five, midfoot, medial heel, and lateral heel. These divisions were visually inspected and manually corrected when needed to ensure accurate representation of the foot's anatomy, as shown in Figure 6.

Given the challenges of differentiating specific forefoot anatomical zones on pedographs due to deformities [65], and the potential biases associated with separating these zones, data from the second to fourth metatarsals were combined into a single category, referred to as the central metatarsals (CMT, Figure 6). The parameters evaluated for each anatomical region during the gait cycle included maximum force (MF, measured in newtons), peak pressure (PP, in kPa), force-time integral (FTI, in Ns), and pressure-time integral (PTI, in kPa).

3.8 Statistical Analysis

Continuous variables, such as radiographic angles and pedobarographic measurements, were expressed as means ± standard deviations, while categorical variables, including lateral head morphology and sesamoid grade, were presented as frequencies and percentages. Comparisons between preoperative and postoperative data within the same group were performed using the paired t-test for normally distributed data or the

doi:10.6342/NTU202501861

Wilcoxon signed-rank test for non-normally distributed data. Categorical variables were analyzed using the Wilcoxon signed-rank test. A p-value ≤ 0.05 (two-tailed) was considered statistically significant. Data were processed and analyzed using SPSS version 17 (SPSS Inc., Chicago, IL, USA).

3.8.1) Sample size estimation

A preliminary power analysis was conducted based on pilot data from five participants. The pilot results indicated a mean reduction in central metatarsal pressure of 22.93 kPa with a standard deviation of 37.92 kPa, leading to an estimated effect size of 0.61. Using a significance level of 0.05 and a statistical power of 80%, the minimum sample size required for adequate comparisons to be 24. To accommodate potential participant dropout and explore additional objectives, the sample size was increased to 30, ensuring sufficient data for robust analysis. All statistical evaluations in this study were carried out using IBM SPSS, version 25 (IBM Corp., Armonk, NY).

3.9 Results

3.9.1) Demographic data

A total of 34 patients, corresponding to 40 feet, met the study's inclusion criteria and underwent isolated MICA performed by the senior author during the designated study period. Of these, one foot was excluded due to ipsilateral brachymetatarsia, two feet were excluded due to prior foot surgeries, and six feet were excluded because of incomplete data. The final analysis comprised 31 feet from 25 patients, including 16 right feet and 15 left feet. Among the participants, 5 were male and 20 were female, with a mean age of 45.61 years and an average body mass index (BMI) of 22.28 kg/m^2 (Table 4).

doi:10.6342/NTU202501861

3.9.2) Radiographic outcomes

Table 5 highlights substantial postoperative enhancements in HVA, IMA, DMAA, 1MTLHS, and LSG, all of which showed statistical significance ($P < 0.001$). The MT1CL was notably shortened by an average of 2.43 mm ($P < 0.001$). However, no significant differences were identified in MT2PD ($P = 0.42$), LMA ($P = 0.44$), or CPA ($P = 0.94$) after the procedure. Additionally, no cases of dorsiflexion malunion were observed at the osteotomy sites.

3.9.3) Pedobarographic outcomes

The pedobarographic data outlined in Tables 6–9 indicate significant decreases in MF, PP, FTI, and PTI within the hallux and first metatarsal regions following MICA ($P < 0.05$). In contrast, no notable changes were observed for these parameters in other forefoot areas.

3.10 Discussion

With the clinical demonstrated success in deformity correction and patient satisfaction[66], the pedobarographic effects following the correction of hallux valgus (HV) using Minimally Invasive Chevron Akin (MICA) osteotomy have not been explored in existing literature. This study identifies key findings indicating that while MICA effectively corrects radiographic parameters in moderate to severe HV cases without associated metatarsalgia, it does not significantly alter central metatarsal loading within three months post-surgery. Notably, reductions in plantar loading over the hallux and first metatarsal head were observed.

MICA has emerged as a widely utilized percutaneous approach for addressing HV due to its rigid fixation and minimally invasive nature.[67] Prior studies[59, 68-72] have demonstrated its effectiveness in improving pain, clinical, and radiological outcomes

doi:10.6342/NTU202501861

over follow-up periods ranging from one to two years or more. These investigations primarily addressed mild to severe HV deformities, and our findings align with these outcomes by confirming MICA's ability to correct structural abnormalities in moderate to severe HV patients. Beyond the commonly assessed parameters such as hallux valgus angle (HVA), intermetatarsal angle (IMA), and distal metatarsal articular angle (DMAA),[59, 68-72] our study highlights additional improvements in 3D deformity correction using metrics like first metatarsal lateral head shape (MT1LHS)[60, 61] and lateral sesamoid grade(LSG)[62]. These insights suggest that MICA may enhance long-term outcomes by lowering recurrence rates through comprehensive 3D corrections.[60, 61].

While the pedobarographic outcomes of various distal metatarsal osteotomy techniques in HV patients have been investigated,[73-79] similar assessments for MICA are absent. Previous reports on distal metatarsal osteotomies have yielded mixed results, with studies showing increased,[73-77], unchanged[78, 79], or decreased[79] plantar loading on central metatarsals. Cancilleri et al.[79] observed reduced central metatarsal loading following distal metatarsal osteotomy, but their cohort exclusively comprised patients with hallux valgus and metatarsalgia. Given that metatarsalgia influences pedobarographic outcomes,[80] the inclusion of such patients likely contributed to their distinct findings. To ensure homogeneity, our study excluded patients with metatarsalgia, enabling us to establish that MICA neither exacerbates nor normalizes central metatarsal loading. These findings suggest that, like other distal metatarsal osteotomies, MICA may not inherently restore optimal foot biomechanics or eliminate risks of metatarsalgia based on pedobarographic assessments.[65, 80-82].

doi:10.6342/NTU202501861

In addition, we identified significant reductions in plantar loading on the hallux and first metatarsal head three months post-MICA. This may indicate diminished functional capacity of the first ray.[41] Although our analysis revealed an average first metatarsal shortening of 2.43 mm, second metatarsal protrusion distance (MT2PD) remained consistent, foot shape appeared unchanged (as evidenced by lateral Meary’s angle and calcaneal pitch angle), and no dorsiflexion malunion was observed. While metatarsal shortening likely contributed to the decreased loading, previous research suggests that reductions within 6 mm are unlikely to impair function.[83] Moreover, Nunes et al.[69] reported satisfactory clinical outcomes despite a 5.1 mm shortening in severe HV cases. Although the observed shortening in our study reached statistical significance, its clinical relevance and implications for plantar loading require further exploration.

This study has several limitations. First, while previous research has reported positive clinical outcomes with MICA,[59, 68-72] our lack of documented clinical scores limits a direct comparison of radiographic, pedobarographic, and functional results. Second, the three-month follow-up period may not fully capture gait adaptations or long-term changes that influence pedobarographic outcomes.[82] Third, our sample size was relatively modest, which, although statistically significant in certain measures, necessitates further validation through larger studies with extended follow-up durations to confirm MICA’s pedobarographic impacts on HV correction.

3.11 Conclusion

The Minimally Invasive Chevron Akin (MICA) technique demonstrates effective correction of radiographic parameters in moderate to severe hallux valgus (HV) patients

doi:10.6342/NTU202501861

without metatarsalgia. However, it does not appear to significantly alter or alleviate central metatarsal loading in this subset of patients.

doi:10.6342/NTU202501861

CHAPTER 4 Study Three: Pedobarographic Analysis of Hallux Valgus and Metatarsus Adductus Surgery

(This study has been submitted and under review currently.)

4.1 Research questions

4.1.1) What is the pedobarographic change of 1st and central metatarsal after surgical correction of HV and MA using MICA and PMMO?

4.1.2) Do the perioperative pedobarographic changes correlate with radiographic changes?

4.2 Study purposes

4.2.1) To report the radiographic and plantar pressure changes of HV and MA correction using MICA and PMMO.

4.2.2) To explore the correlation of perioperative radiographic and plantar pressure changes of HV and MA correction using MICA and PMMO.

4.3 Hypothesis

The null hypotheses of this study are:

4.3.1) There is no statistically significant changes in plantar pressure after HV and MA correction using MICA and PMMO.

4.4 Study design (Figure 7)

The present investigation was conducted as a single-center, prospective cohort, receiving approval from the Institutional Review Board of Changhua Show Chwan

doi:10.6342/NTU202501861

Memorial Hospital (SCMH_IRB-1130408, see Appendix 3). The study adhered strictly to the guidelines set forth by the Health Insurance Portability and Accountability Act and the principles outlined in the Declaration of Helsinki.

4.5 Participants

All individuals meeting the inclusion and exclusion criteria underwent treatment with the 4th generation MICA[56] without any supplementary procedures on the lesser toes. These patients were then followed up for review.

4.5.1) Inclusion criteria

Patient with moderate to severe HV (HV angle > 20° or intermetatarsal angle > 13°)[57, 58] and MA (Sgarlato's angle > 15°)[84], who exhibited metatarsalgia mandatory to surgical treatment, and was aged over 18.

4.5.2) Exclusion criteria

Patients presenting with ipsilateral foot conditions other than HV and MA—including first tarsometatarsal joint hypermobility, pes planus, or a Sgarlato's angle of less than 15°—were excluded from the study. The exclusion criteria also encompassed individuals with a history of lower limb surgeries, diagnosed rheumatic disorders, or incomplete datasets.

4.6 Surgical techniques and postoperative protocols

4.6.1) Minimally Invasive Chevron Akin (MICA)

As described in chapter 3.

doi:10.6342/NTU202501861

4.6.2) Proximal Metatarsal Minimally invasive Osteotomy (PMMO)

The patient was put under supine position with a bump placed under the operative knee to keep knee flexion. The tourniquet was applied on the thigh and the pressure was set at 280mmHg. A stab wound was made over dorsal foot superficial to proximal metaphyseal region of 2nd-4th metatarsals. Percutaneous oblique osteotomies at proximal meta-diaphyseal region of 2nd-4th metatarsals were done under fluoroscopic guidance. In axial view, the osteotomy goes from distal 2nd metatarsal to proximal 4th metatarsal. In sagittal view, the osteotomy goes about half of the angle between the floor and the line perpendicular to the metatarsal axis.（Figure 8）

4.6.3) Postoperative protocol

Following surgery, patients were instructed to use a soft hallux valgus brace (Bunion Adjustable Splint, DARCO Co.) in combination with a rigid-soled orthopedic shoe for six weeks. After this period, they were permitted to transition to comfortable footwear of their own choice without any restrictions. Immediate full weight-bearing was allowed postoperatively.

4.7 Data Collection

4.7.1) Radiographic parameters

Radiographic assessments were conducted using weight-bearing radiographs obtained prior to surgery and at the six-month postoperative follow-up. Key parameters documented included the hallux valgus angle (HVA), intermetatarsal angle (IMA), and the metatarsal adductus angle evaluated according to Sgarlato’s technique.[84]

doi:10.6342/NTU202501861

4.7.2) Pedobarographic parameters

As described in chapter 3.

4.8 Statistical Analysis

The statistical analysis was conducted using a paired t-test for parametric data and the Wilcoxon signed-rank test for non-parametric data. A two-tailed p-value of less than 0.05 was considered statistically significant. All data were analyzed using IBM SPSS Statistics for Windows, version 24 (IBM Corporation, Armonk, NY, USA).

4.8.1) Sample size estimation

A preliminary analysis involving five patients was conducted to perform an a priori power analysis. The pilot data revealed an effect size of 1.98, calculated using the mean reduction and standard deviation of central metatarsal pressure before and after surgery, which were 75.4 kPa and 38.5 kPa, respectively. Although the pilot yielded $g = 1.98$, a conservative target of 1.0 was adopted to mitigate over-estimation. With a significance level set at 0.05 and a power of 0.80, the required sample size for adequate statistical comparison was estimated to be 20 participants. All data analyses in this study were performed using IBM SPSS Statistics, version 25 (IBM Corp., Armonk, NY, USA).

4.9 Results

Twenty-five patients were included in this study, comprising 6 males and 19 females, with an average age of 50.1 years. The mean skin-to-skin operation time was 47.2 minutes, and the average hospital stay was 3.6 days. The average time to complete bone union is 189 days. (Table 10)

doi:10.6342/NTU202501861

The hallux valgus angle (HVA), intermetatarsal angle (IMA), and metatarsus adductus (MA) angle, measured using the Sgarlato and modified Sgarlato methods, demonstrated significant improvement following surgery (Table 11).

Postoperative analysis revealed significant shortening in the proximal phalanx of hallux(P1) and the second to fourth metatarsals (M2–M4). First metatarsal (M1) shortening was observed after osteotomy but no statistic significant. The mean shortening lengths for P1, M1, M2, M3, and M4 were 2.7 mm, 5.4 mm, 7.1 mm, 7.3 mm, and 5.8 mm, respectively (Table 12).

As for the pedobarographic outcomes, the maximum force, peak pressure, force-time interval, and pressure-time interval significantly decreased in T1, T2-5, M2-4 regions postoperatively. While all pedobarographic parameters increased in M1 and M5 regions postoperatively (Table 13-16).

4.10 Discussion

The Minimally Invasive Chevron and Akin (MICA) technique has proven to be a reliable method for treating hallux valgus, demonstrating improvements in both clinical and radiological outcomes with a lower recurrence rate[68]. Our study showed that the combination of MICA and proximal metatarsal medializing osteotomy (PMMO) is an effective approach for managing hallux valgus with metatarsus adductus. Postoperatively, significant corrections of the hallux valgus angle (HVA), intermetatarsal angle (IMA), and metatarsus adductus (MA) were observed.

Hallux valgus with metatarsus adductus presents a complex challenge for surgeons, and there is currently no consensus regarding the optimal surgical approach in terms of outcomes, recurrence rates, and complications. Larholt and Kilmartin [36] proposed a method that addresses HV without involving the lesser metatarsals. However, their results

doi:10.6342/NTU202501861

showed that 42% of patients had residual HVA exceeding 15° at the final follow-up. This highlights the potential need for a more comprehensive surgical approach that includes lesser metatarsal procedures.

Jyoti Sharma et al. [37] introduced a detailed algorithm in 2015 for HV with severe MA, which required 6 weeks of non-weight bearing postoperatively. In 2019, Hiroaki Shima used proximal crescentic osteotomy combined with proximal abduction osteotomies, indicating 4 weeks of non-weight bearing and full weight bearing by 7 weeks [85]. Anna-Kathrin Leucht et al. described the use of first-second-third tarsometatarsal (TMT) fusion to treat HV with severe MA and associated TMT arthritis, though their study did not specify postoperative protocols [86].

With the growing adoption of minimally invasive surgery (MIS) techniques, such as MICA combined with PMMO[38] or DMMO[39], patients benefit from reduced soft tissue trauma and faster recovery. These procedures allow full weight-bearing immediately after recovery from anesthesia. However, prior MIS studies [38, 39] involved small patient cohorts. Our study, although limited by a small cohort, is the first to include 25 patients treated for HV with MA using MICA combined with PMMO.

Duo Wai-Chi Wong et al. [41] conducted a systematic review and meta-analysis of forefoot function following HV surgery, analysing 20 studies involving various surgical techniques. They found that hallux load decreased while impulse increased in the central metatarsals postoperatively, even when no lesser metatarsal procedures were performed. HV surgery that does not address the lesser metatarsals tends to increase peak pressure and impulse on the second to fourth metatarsals (M2–M4). Hsu et al. [55] investigated the plantar pressure changes after MICA also suggested that central metatarsal pressure was unchanged after MICA along. Neunteufel et al.[87] found that after DMMO, peak plantar pressure decreased in the second and third metatarsophalangeal (MTP) joints

doi:10.6342/NTU202501861

while increasing medially and laterally. Kosho Togei et al. [63] used proximal crescentic osteotomy of the first metatarsal with proximal shortening osteotomy of the lesser metatarsals in patients with HV and metatarsalgia, reporting significant decreases in peak pressure under the second metatarsal head.

Our study examined foot pressure changes following MICA combined with PMMO. We observed significant decreases in MF, PP, FTI, and PTI on M2–4 postoperatively. Conversely, MF, PP, FTI, and PTI increased on M1 and M5, although these changes were not statistically significant. This suggests partial restoration of forefoot function.

We also evaluated metatarsal length changes after osteotomy. Simple DMMO can achieve shortening of 3–7 mm in the lesser metatarsals [88, 89]. Previous studies reported approximately 4 mm of shortening in M2–4 in patients with HV and MA treated with lateralizing DMMO [90]. In our study, PMMO resulted in significant shortening of 5–7 mm in M2–4. Although M1 also shortened postoperatively, this change was not statistically significant. The relative lengthening of M1 and M5 may contribute to the increased MF, PP, FTI, and PTI observed in these regions.

Lewis et al. [68] reported a case series of 333 feet treated with third-generation MICA for HV, with an overall complication rate of 21.3%. The rates of delayed union, nonunion, and malunion were 2.7%, while the screw removal rate was 6.3%. Complication data for PMMO are limited. Previous studies on DMMO [88, 91] reported nonunion and metatarsal head necrosis as potential complications. Nonunion was more likely when the osteotomy was performed too proximally or with a sagittal cutting angle exceeding 45°, while metatarsal head necrosis was associated with distal osteotomies or sagittal cutting angles less than 45°[91]. In our study, one delay union (11.5 months) was observed. No screw removed at the final follow up.

doi:10.6342/NTU202501861

This study has several limitations. First, clinical outcomes, such as pain scores, functional assessments, and patient satisfaction, were not collected, precluding a comprehensive analysis. Second, the small sample size may introduce bias. Further studies with larger cohorts and extended follow-up periods are necessary to validate our findings.

4.11 Conclusion

The combination of MICA and PMMO is an effective surgical method for treating HV with MA. Hallux valgus surgery combine lesser metatarsal procedure like PMMO can redistribute the pressure over forefoot.

doi:10.6342/NTU202501861

Chapter 5 General Conclusion

This dissertation presents three studies that explore how minimally invasive surgery affects foot structure and function. All studies show that MIS can correct foot deformities and improve clinical scores. But more importantly, they also show how foot pressure patterns change after surgery. These pressure changes help us understand the mechanical results of the surgery beyond just the X-ray images.

From the viewpoint of both a surgeon and a physical therapy researcher, I believe this type of combined analysis is necessary. Surgery changes the shape of the foot, but recovery of function also depends on how the foot handles weight during walking. Plantar pressure analysis gives us a way to measure this. In the future, combining surgical planning with biomechanical data can help create better rehabilitation programs. This work is an important step toward connecting surgical outcomes with physical function, helping both surgeons and therapists provide better care for patients with foot deformities.

doi:10.6342/NTU202501861

REFERENCES

1. Rome, K., R.L. Ashford, and A. Evans, *Non-surgical interventions for paediatric pes planus.* Cochrane Database Syst Rev, 2010(7): p. CD006311.
2. Tahririan, M.A., S. Ramtin, and P. Taheri, *Functional and radiographic comparison of subtalar arthroereisis and lateral calcaneal lengthening in the surgical treatment of flexible flatfoot in children.* Int Orthop, 2021. **45**(9): p. 2291-2298.
3. Smith, C., et al., *Subtalar arthroereisis for the treatment of the symptomatic paediatric flexible pes planus: a systematic review.* EFORT Open Rev, 2021. **6**(2): p. 118-129.
4. Bernasconi, A., F. Lintz, and F. Sadile, *The role of arthroereisis of the subtalar joint for flatfoot in children and adults.* EFORT Open Rev, 2017. **2**(11): p. 438-446.
5. Metcalfe, S.A., F.L. Bowling, and N.D. Reeves, *Subtalar joint arthroereisis in the management of pediatric flexible flatfoot: a critical review of the literature.* Foot Ankle Int, 2011. **32**(12): p. 1127-39.
6. Tan, J.H.I., et al., *The outcomes of subtalar arthroereisis in pes planus: a systemic review and meta-analysis.* Arch Orthop Trauma Surg, 2021. **141**(5): p. 761-773.
7. Ruiz-Picazo, D., et al., *Radiographic and Functional Results following Subtalar Arthroereisis in Pediatric Flexible Flatfoot.* Adv Orthop, 2019. **2019**: p. 5061934.
8. Mazzotti, A., et al., *Long-term results of subtalar arthroereisis for the treatment of symptomatic flexible flatfoot in children: an average fifteen year follow-up study.* Int Orthop, 2021. **45**(3): p. 657-664.
9. Shi, G.G.W., J.L.; Turner, N.S., 3rd; Kitaoka, H.B., *Operative Approach to Adult Hallux Valgus Deformity: Principles and Techniques.* J Am Acad Orthop Surg, 2020. **28**: p. 410-418.
10. Lopez, V.S., G., *Metatarsalgia: Assessment Algorithm and Decision Making.* Foot Ankle Clin, 2019. **24**.
11. Nunes, G.A.d.C., K.A.M.; Ferreira, G.F.; Filho, M.V.P.; Baptista, A.D.; Zambelli, R.; Vega, J., *Minimally invasive Chevron Akin (MICA) osteotomy for severe hallux valgus.* Arch Orthop Trauma Surg, 2023(143): p. 5507-5517.
12. Lewis, T.L.R., R.; Miller, G.; Gordon, D.J., *Third-Generation Minimally Invasive Chevron and Akin Osteotomies (MICA) in Hallux Valgus Surgery: Two-Year Follow-up of 292 Cases.* J Bone Joint Surg Am, 2021(103): p. 1203-1211.
13. Razak, A.H.Z., A.; Begg, R.K.; Wahab, Y., *Foot plantar pressure measurement system: a review.* Sensors (Basel), 2012(12): p. 9884-9912.
14. Wafai, L.Z., A.; Woulfe, J.; Aziz, S.M.; Begg, R., *Identification of Foot Pathologies Based on Plantar Pressure Asymmetry.* Sensors (Basel), 2015(15): p. 20392-20408.
15. Deepashini, H.O., B.; Paungmali, A.; Amaramalar, N.; Ohnmar, H.; Leonard, J., *An insight into the plantar pressure distribution of the foot in clinical practice: Narrative review.* Polish Annals of Medicine, 2014(21): p. 51-56.
16. Bryant, A.R.T., P.; Cole, J.H, *Plantar pressure and radiographic changes to the forefoot after the Austin bunionectomy.* J Am Podiatr Med Assoc, 2005(95): p. 357-365.
17. Hida, T.O., R.; Yasuda, T.; Jotoku, T.; Shima, H, *Comparison of plantar pressure distribution in patients with hallux valgus and healthy matched controls.* J Orthop Sci, 2017(22): p. 1054-1059.
18. Hofmann, U.K.G., M.; Wiesenreiter, K.; Müller, O.; Wünschel, M.; Mittag, F., *Transfer of plantar pressure from the medial to the central forefoot in patients with hallux valgus.* BMC Musculoskelet Disord, 2019(20): p. 149.

doi:10.6342/NTU202501861

19. Wong, D.W.C., J.C.; Zhao, J.G.; Ni, M.; Yang, Z.Y., *Forefoot Function after Hallux Valgus Surgery: A Systematic Review and Meta-Analysis on Plantar Load Measurement.* J Clin Med, 2023(12).
20. Verdu-Roman, C.S.-R., J.; Martinez-Gimenez, E.; Carratala-Munuera, C.; Lopez-Pineda, A., *Plantar pressure improvement in moderate hallux valgus with modified chevron osteotomy: Clinical and radiographic outcomes.* Foot Ankle Surg, 2020(26): p. 205-208.
21. Kernozek, T.W.S., S.A., *Chevron (Austin) distal metatarsal osteotomy for hallux valgus: comparison of pre- and post-surgical characteristics.* Foot Ankle Int, 2002. **23**.
22. Costa, J.A., A.; Kleinowski, D.; Kroth, L.; Contreras, M., *Modified Chevron osteotomy: preliminary analysis of baropodometric behavior.* Acta Ortopédica Brasileira, 2009(18): p. 191-196.
23. Resch, S.S., A., *Evaluation of hallux valgus surgery with dynamic foot pressure registration with the Fscan system.* The Foot, 1995(5): p. 115-121.
24. Mazzotti, A.A., A.; Artioli, E.; Langone, L.; Zielli, S.O.; Martini, B.; Traina, F.; Faldini, C.; Brognara, L., *Hallux Valgus Plantar Pressure Distribution before and after a Distal Metatarsal Osteotomy.* J Clin Med, 2024(13).
25. King, C.M.H., G.A.; Ford, L.A., *Effects of the lapidus arthrodesis and chevron bunionectomy on plantar forefoot pressures.* J Foot Ankle Surg, 2014(53): p. 415-419.
26. Cancilleri, F.M., A.; Martinelli, N.; Ippolito, M.; Spiezia, F.; Ronconi, P.; Denaro, V. , *Comparison of plantar pressure, clinical, and radiographic changes of the forefoot after biplanar Austin osteotomy and triplanar Boc osteotomy in patients with mild hallux valgus.* Foot Ankle Int, 2008(29): p. 817-824.
27. Brodsky, J.W.B., A.D.; Robinson, A.H.; Westra, S.; Negrine, J.P.; Shabat, S., *Surgery for hallux valgus with proximal crescentic osteotomy causes variable postoperative pressure patterns.* Clin Orthop Relat Res, 2006(443): p. 280-286.
28. Moerenhout, K.C., S.; Crevoisier, X., *Outcome of the modified Lapidus procedure for hallux valgus deformity during the first year following surgery: A prospective clinical and gait analysis study.* Clinical Biomechanics, 2019(61): p. 205-210.
29. Lewis, T.L.L., B.; Alkhalfan, Y.; Trowbridge, S.; Gordon, D.; Vernois, J.; Lam, P.; Ray, R., *Fourth-Generation Minimally Invasive Hallux Valgus Surgery With Metaphyseal Extra-Articular Transverse and Akin Osteotomy (META): 12 Month Clinical and Radiologic Results.* Foot Ankle Int, 2023(44): p. 178-191.
30. de Carvalho, K.A.M.B., A.D.; de Cesar Netto, C.; Johnson, A.H.; Dalmau-Pastor, M. , *Minimally Invasive Chevron-Akin for Correction of Moderate and Severe Hallux Valgus Deformities: Clinical and Radiologic Outcomes With a Minimum 2-Year Follow-up.* Foot Ankle Int, 2022(43): p. 1317-1330.
31. Tay, A.Y.W.G., G.S.; Koo, K.; Yeo, N.E.M., *Third-Generation Minimally Invasive Chevron-Akin Osteotomy for Hallux Valgus Produces Similar Clinical and Radiological Outcomes as Scarf-Akin Osteotomy at 2 Years: A Matched Cohort Study.* Foot Ankle Int, 2022(43): p. 321-330.
32. Holme, T.J.S., S.S.; Patel, B.; Kunasingam, K., *Third-Generation Minimally Invasive Chevron Akin Osteotomy for Hallux Valgus.* Foot Ankle Int, 2020(41): p. 50-56.
33. Waldecker, U., *Metatarsalgia in hallux valgus deformity: a pedobarographic analysis.* J Foot Ankle Surg, 2002(41): p. 300-308.
34. Noback, P.C.T., D.P.; Vosseller, J.T., *Republication of "Evidence Versus Practice: Operative Treatment Preferences in Hallux Valgus".* Foot Ankle Orthop, 2023(8).
35. Choi, S.M., et al., *Effect of Metatarsus Adductus on Hallux Valgus Treated With Proximal Reverse Chevron Metatarsal Osteotomy.* Foot Ankle Int, 2021. **42**(7): p. 886-893.

doi:10.6342/NTU202501861

36. Larholt, J. and T.E. Kilmartin, *Rotational scarf and akin osteotomy for correction of hallux valgus associated with metatarsus adductus.* Foot Ankle Int, 2010. **31**(3): p. 220-8.
37. Sharma, J. and U. Aydogan, *Algorithm for Severe Hallux Valgus Associated With Metatarsus Adductus.* Foot Ankle Int, 2015. **36**(12): p. 1499-503.
38. Burg, A. and E. Palmanovich, *Correction of Severe Hallux Valgus with Metatarsal Adductus Applying the Concepts of Minimally Invasive Surgery.* Foot Ankle Clin, 2020. **25**(2): p. 337-343.
39. Kurashige, T., *Minimally invasive surgery for severe hallux valgus with severe metatarsus adductus: Case reports.* Foot & Ankle Surgery: Techniques, Reports & Cases, 2021. **1**(1).
40. Koller, U., et al., *Plantar pressure characteristics in hallux valgus feet.* J Orthop Res, 2014. **32**(12): p. 1688-93.
41. Wong, D.W., et al., *Forefoot Function after Hallux Valgus Surgery: A Systematic Review and Meta-Analysis on Plantar Load Measurement.* J Clin Med, 2023. **12**(4).
42. Fishco, W.D., M.B. Ellis, and M.W. Cornwall, *Influence of a metatarsus adductus foot type on plantar pressures during walking in adults using a pedobarograph.* J Foot Ankle Surg, 2015. **54**(3): p. 449-53.
43. Wang JH, C.C., Chuang HC, Chen YY, *Long-term results of subtalar arthroereisis for symptomatic flexible flatfoot in paediatrics.* Int Orthop, 2025. **49**(5): p. 1175-1183.
44. Mazzotti, A., et al., *Subtalar arthroereisis post-operative management in children: A literature review.* Foot (Edinb), 2023. **56**: p. 102037.
45. Indino, C., et al., *Effectiveness of subtalar arthroereisis with endorthesis for pediatric flexible flat foot: a retrospective cross-sectional study with final follow up at skeletal maturity.* Foot Ankle Surg, 2020. **26**(1): p. 98-104.
46. Memeo, A., et al., *Flexible Juvenile Flat Foot Surgical Correction: A Comparison Between Two Techniques After Ten Years' Experience.* J Foot Ankle Surg, 2019. **58**(2): p. 203-207.
47. Megremis, P. and O. Megremis, *Arthroereisis for Symptomatic Flexible Flatfoot Deformity in Young Children: Radiological Assessment and Short-Term Follow-Up.* J Foot Ankle Surg, 2019. **58**(5): p. 904-915.
48. Wang, S., et al., *Mid-term Results of Subtalar Arthroereisis with Talar-Fit Implant in Pediatric Flexible Flatfoot and Identifying the Effects of Adjunctive Procedures and Risk Factors for Sinus Tarsi Pain.* Orthop Surg, 2021. **13**(1): p. 175-184.
49. Neves, J.C.J., et al., *Intra- and Inter-Examiner Reliability of the Viladot Method in Children.* J Manipulative Physiol Ther, 2021. **44**(1): p. 56-60.
50. Vogt, B., et al., *Subtalar Arthroereisis for Flexible Flatfoot in Children-Clinical, Radiographic and Pedobarographic Outcome Comparing Three Different Methods.* Children (Basel), 2021. **8**(5).
51. Szesz, A., et al., *An evaluation of subtalar titanium screw arthroereisis for the treatment of symptomatic paediatric flatfeet - early results.* BMC Musculoskelet Disord, 2023. **24**(1): p. 825.
52. Moraca G, M.N., Bianchi A, Filardo G, Sansone V, *Subtalar arthroereisis with metallic implant is a safe and effective treatment for pediatric patients with symptomatic flexible flatfeet. A 10-year clinical and radiographic follow-up.* Foot Ankle Surg, 2025. **31**(1): p. 31-37.
53. Cook, E.A., J.J. Cook, and P. Basile, *Identifying risk factors in subtalar arthroereisis explantation: a propensity-matched analysis.* J Foot Ankle Surg, 2011. **50**(4): p. 395-401.
54. Prachgosin, T., et al., *Medial longitudinal arch biomechanics evaluation during gait in subjects with flexible flatfoot.* Acta Bioeng Biomech, 2015. **17**(4): p. 121-30.

doi:10.6342/NTU202501861

55. Hsu, W.K., et al., *Minimally Invasive Chevron Akin (MICA) Osteotomy Corrects Radiographic Parameters but Not Central Metatarsal Loading in Moderate to Severe Hallux Valgus without Metatarsalgia.* Life (Basel), 2024. **14**(6).
56. Redfern, D. and J. Vernois, *Minimally Invasive Chevron Akin (MICA) for Correction of Hallux Valgus.* Techniques in Foot & Ankle Surgery, 2016. **15**(1): p. 3-11.
57. Coughlin, M.J. and C.P. Jones, *Hallux valgus: demographics, etiology, and radiographic assessment.* Foot Ankle Int, 2007. **28**(7): p. 759-77.
58. Shi, G.G., et al., *Operative Approach to Adult Hallux Valgus Deformity: Principles and Techniques.* J Am Acad Orthop Surg, 2020. **28**(10): p. 410-418.
59. Lewis, T.L., et al., *Fourth-Generation Minimally Invasive Hallux Valgus Surgery With Metaphyseal Extra-Articular Transverse and Akin Osteotomy (META): 12 Month Clinical and Radiologic Results.* Foot Ankle Int, 2023. **44**(3): p. 178-191.
60. Okuda, R., et al., *The shape of the lateral edge of the first metatarsal head as a risk factor for recurrence of hallux valgus.* J Bone Joint Surg Am, 2007. **89**(10): p. 2163-72.
61. Wagner, P. and E. Wagner, *Role of Coronal Plane Malalignment in Hallux Valgus Correction.* Foot Ankle Clin, 2020. **25**(1): p. 69-77.
62. Agrawal, Y., A. Desai, and J. Mehta, *Lateral sesamoid position in hallux valgus: correlation with the conventional radiological assessment.* Foot Ankle Surg, 2011. **17**(4): p. 308-11.
63. Togei, K., et al., *Plantar pressure distribution in hallux valgus feet after a first metatarsal proximal crescentic osteotomy with a lesser metatarsal proximal shortening osteotomy.* Foot Ankle Surg, 2021. **27**(6): p. 665-672.
64. Bryant, A., K. Singer, and P. Tinley, *Comparison of the reliability of plantar pressure measurements using the two-step and midgait methods of data collection.* Foot Ankle Int, 1999. **20**(10): p. 646-50.
65. Hofmann, U.K., et al., *Transfer of plantar pressure from the medial to the central forefoot in patients with hallux valgus.* BMC Musculoskelet Disord, 2019. **20**(1): p. 149.
66. P Ruberto, S.C., G Bocchino, A Giuliani, R Vitiello, F Forconi, G Malerba, G Maccauro, *Utilisation of the minimally invasive chevron akin (mica) osteotomy for severe hallux valgus: a systematic review.* Musculoskelet Surg, 2025. **109**(2): p. 133-143.
67. Lai, M.C., et al., *Clinical and Radiological Outcomes Comparing Percutaneous Chevron-Akin Osteotomies vs Open Scarf-Akin Osteotomies for Hallux Valgus.* Foot Ankle Int, 2018. **39**(3): p. 311-317.
68. Lewis, T.L., et al., *Third-Generation Minimally Invasive Chevron and Akin Osteotomies (MICA) in Hallux Valgus Surgery: Two-Year Follow-up of 292 Cases.* J Bone Joint Surg Am, 2021. **103**(13): p. 1203-1211.
69. Nunes, G.A., et al., *Minimally invasive Chevron Akin (MICA) osteotomy for severe hallux valgus.* Arch Orthop Trauma Surg, 2023. **143**(9): p. 5507-5514.
70. de Carvalho, K.A.M., et al., *Minimally Invasive Chevron-Akin for Correction of Moderate and Severe Hallux Valgus Deformities: Clinical and Radiologic Outcomes With a Minimum 2-Year Follow-up.* Foot Ankle Int, 2022. **43**(10): p. 1317-1330.
71. Tay, A.Y.W., et al., *Third-Generation Minimally Invasive Chevron-Akin Osteotomy for Hallux Valgus Produces Similar Clinical and Radiological Outcomes as Scarf-Akin Osteotomy at 2 Years: A Matched Cohort Study.* Foot Ankle Int, 2022. **43**(3): p. 321-330.
72. Holme, T.J., et al., *Third-Generation Minimally Invasive Chevron Akin Osteotomy for Hallux Valgus.* Foot Ankle Int, 2020. **41**(1): p. 50-56.
73. Verdu-Roman, C., et al., *Plantar pressure improvement in moderate hallux valgus with modified chevron osteotomy: Clinical and radiographic outcomes.* Foot Ankle Surg, 2020. **26**(2): p. 205-208.

doi:10.6342/NTU202501861

74. Kernozek, T.W. and S.A. Sterriker, *Chevron (Austin) distal metatarsal osteotomy for hallux valgus: comparison of pre- and post-surgical characteristics.* Foot Ankle Int, 2002. **23**(6): p. 503-8.
75. Costa, J., et al., *Modified Chevron osteotomy: preliminary analysis of baropodometric behavior.* Acta Ortopédica Brasileira, 2009. **18**: p. 191-196.
76. Resch, S. and A. Stenström, *Evaluation of hallux valgus surgery with dynamic foot pressure registration with the Fscan system.* The Foot, 1995. **5**(3): p. 115-121.
77. Mazzotti, A., et al., *Hallux Valgus Plantar Pressure Distribution before and after a Distal Metatarsal Osteotomy.* J Clin Med, 2024. **13**(6).
78. King, C.M., G.A. Hamilton, and L.A. Ford, *Effects of the lapidus arthrodesis and chevron bunionectomy on plantar forefoot pressures.* J Foot Ankle Surg, 2014. **53**(4): p. 415-9.
79. Cancilleri, F., et al., *Comparison of plantar pressure, clinical, and radiographic changes of the forefoot after biplanar Austin osteotomy and triplanar Boc osteotomy in patients with mild hallux valgus.* Foot Ankle Int, 2008. **29**(8): p. 817-24.
80. Waldecker, U., *Metatarsalgia in hallux valgus deformity: a pedobarographic analysis.* J Foot Ankle Surg, 2002. **41**(5): p. 300-8.
81. Hida, T., et al., *Comparison of plantar pressure distribution in patients with hallux valgus and healthy matched controls.* J Orthop Sci, 2017. **22**(6): p. 1054-1059.
82. Bryant, A.R., P. Tinley, and J.H. Cole, *Plantar pressure and radiographic changes to the forefoot after the Austin bunionectomy.* J Am Podiatr Med Assoc, 2005. **95**(4): p. 357-65.
83. Geng, X., et al., *Impact of first metatarsal shortening on forefoot loading pattern: a finite element model study.* BMC Musculoskelet Disord, 2019. **20**(1): p. 625.
84. E Engel, N.E., I Krems, *A simplified metatarsus adductus angle.* J Am Podiatry Assoc, 1983(73): p. 620-628.
85. Shima, H., et al., *Operative Treatment for Hallux Valgus With Moderate to Severe Metatarsus Adductus.* Foot Ankle Int, 2019. **40**(6): p. 641-647.
86. Leucht, A.K., et al., *The Windswept Foot: Dealing with Metatarsus Adductus and Toe Valgus.* Foot Ankle Clin, 2020. **25**(3): p. 413-424.
87. Neunteufel, E., et al., *Minimally Invasive Distal Metatarsal Metaphyseal Osteotomy of the Lesser Toes: Clinical, Radiologic, and Pedobarographic Outcomes.* Foot Ankle Int, 2022. **43**(2): p. 153-163.
88. Ferraz Ferreira, G., et al., *Distal Metatarsal Metaphyseal Osteotomy (DMMO) for lesser toe metatarsalgia: a case series of 195 osteotomies.* Journal of the Foot & Ankle, 2022. **16**(2): p. 153-156.
89. Malhotra, K., et al., *Minimally invasive distal metaphyseal metatarsal osteotomy (DMMO) for symptomatic forefoot pathology - Short to medium term outcomes from a retrospective case series.* Foot (Edinb), 2019. **38**: p. 43-49.
90. Chomej, P., et al., *Lateralising DMMO (MIS) for simultaneous correction of a pes adductus during surgical treatment of a hallux valgus.* Foot (Edinb), 2020. **45**: p. 101722.
91. Krenn, S., et al., *Minimally Invasive Distal Metatarsal Metaphyseal Osteotomy of the Lesser Toes: Learning Curve.* Foot Ankle Spec, 2018. **11**(3): p. 263-268.

doi:10.6342/NTU202501861

FIGURES

Figure 1: Illustration of the study design of Study 1.

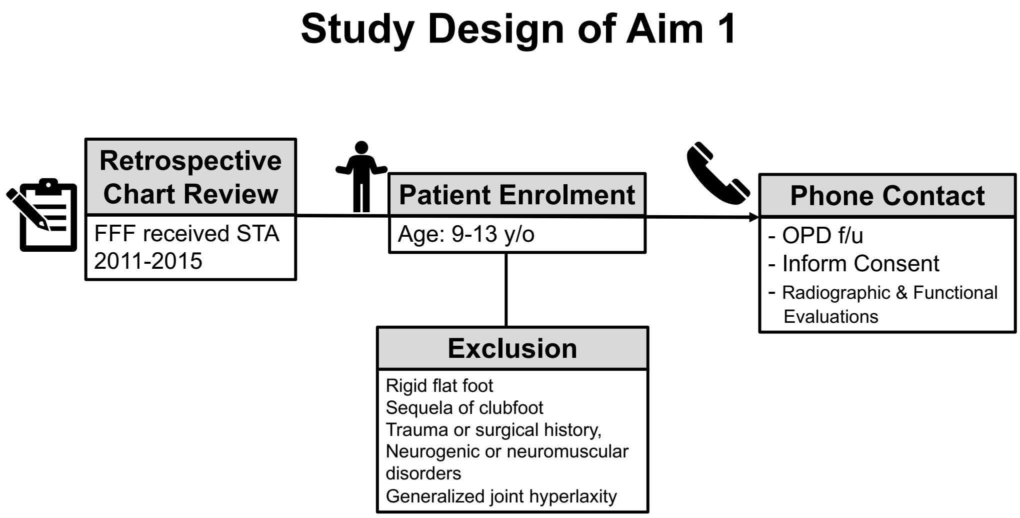

doi:10.6342/NTU202501861

Figure 2: Radiographs of subtalar arthroereisis before, during, and after the surgery. The upper section of the figure illustrates intraoperative radiographs captured during the subtalar arthroereisis procedure. The lower section presents weight-bearing lateral radiographs of the same foot, showcasing preoperative and postoperative states. The yellow lines denote the Meary's angle (lateral talar–1st metatarsal angle), clearly demonstrating significant correction in foot alignment when comparing the preoperative and postoperative images.

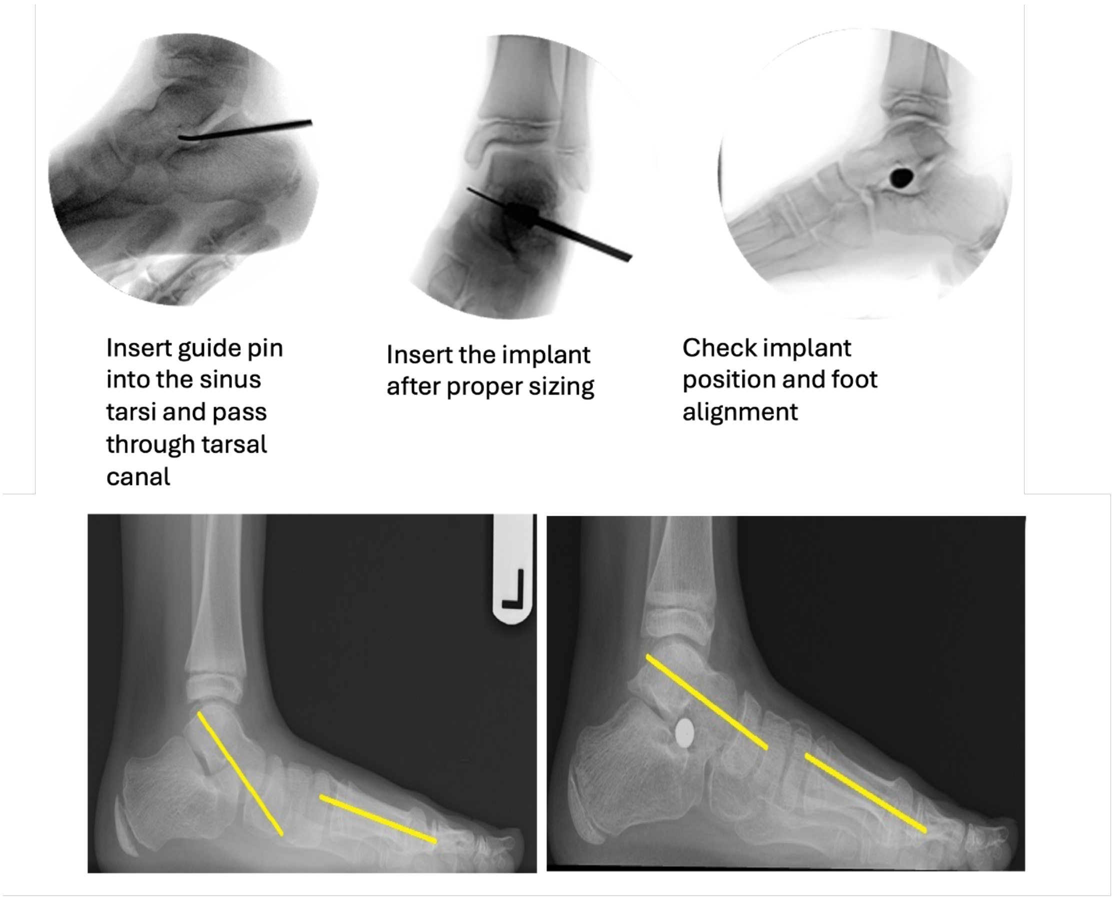

doi:10.6342/NTU202501861

Figure 3: Radiographic parameters relavent to flat foot deformity.

Left: weight-bearing antero-posterior view of right foot. (A) talonavicular coverage. angle (B) Antero-posterior talar–1st metatarsal angle (C) Antero-posterior talocalcaneal angle (Kite’s angle).

Middle: weight-bearing antero-posterior (AP) ankle mortise radiograph showed. fibular axis calcaneal offset (FACO)

Right: weight-bearing lateral foot radiograph. (A) Lateral talar–1st metatarsal angle (Meary’s angle) (B) Calcaneal inclination (C) Lateral talocalcaneal angle (D). Moreau-Costa-Bartani angle (E) Talar declination.

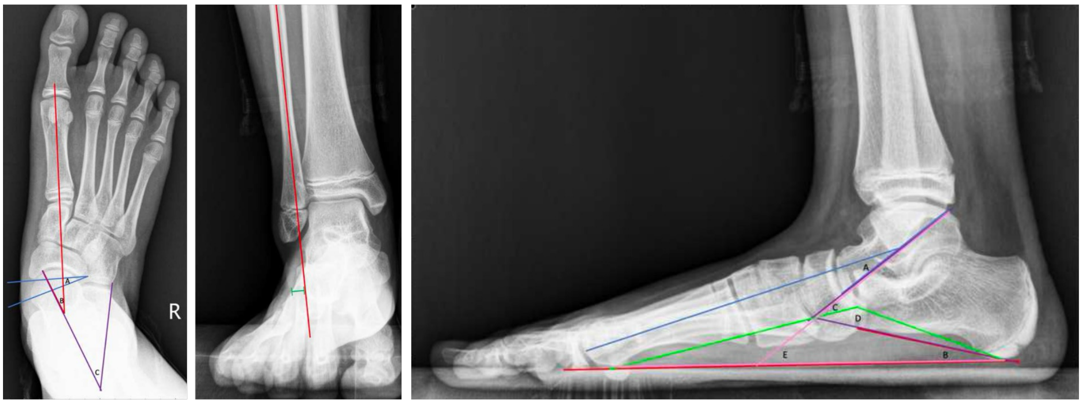

doi:10.6342/NTU202501861

Figure 4: Illustration of the study design of study 2.

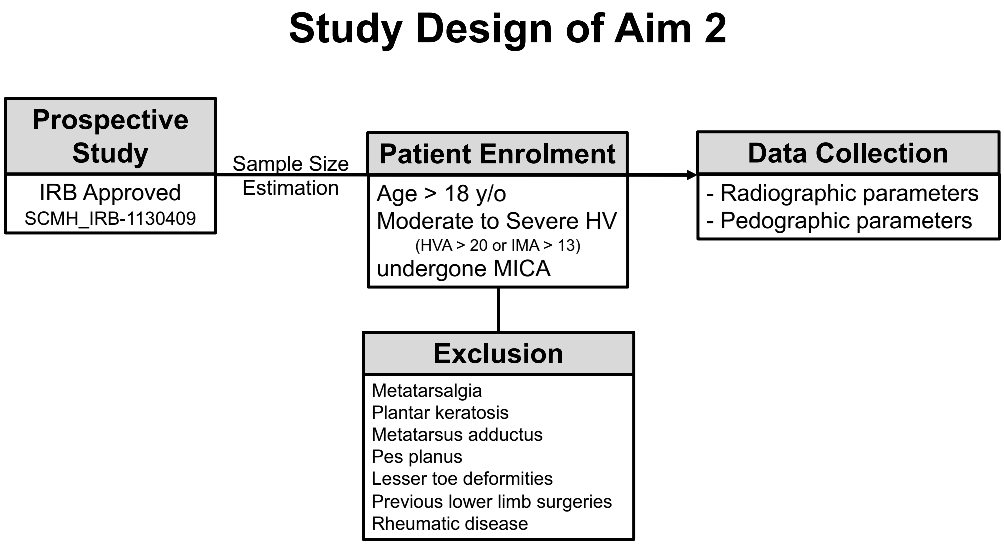

doi:10.6342/NTU202501861

Figure 5: Minimally Invasive Chevron Akin (MICA) osteotomy for hallux valgus correction.

The upper radiographs showed the intra-operative radiographs of MICA.

The lower radiographs showed a patient with hallux valgus receiving MICA before (left) and three months after (right) the surgery.

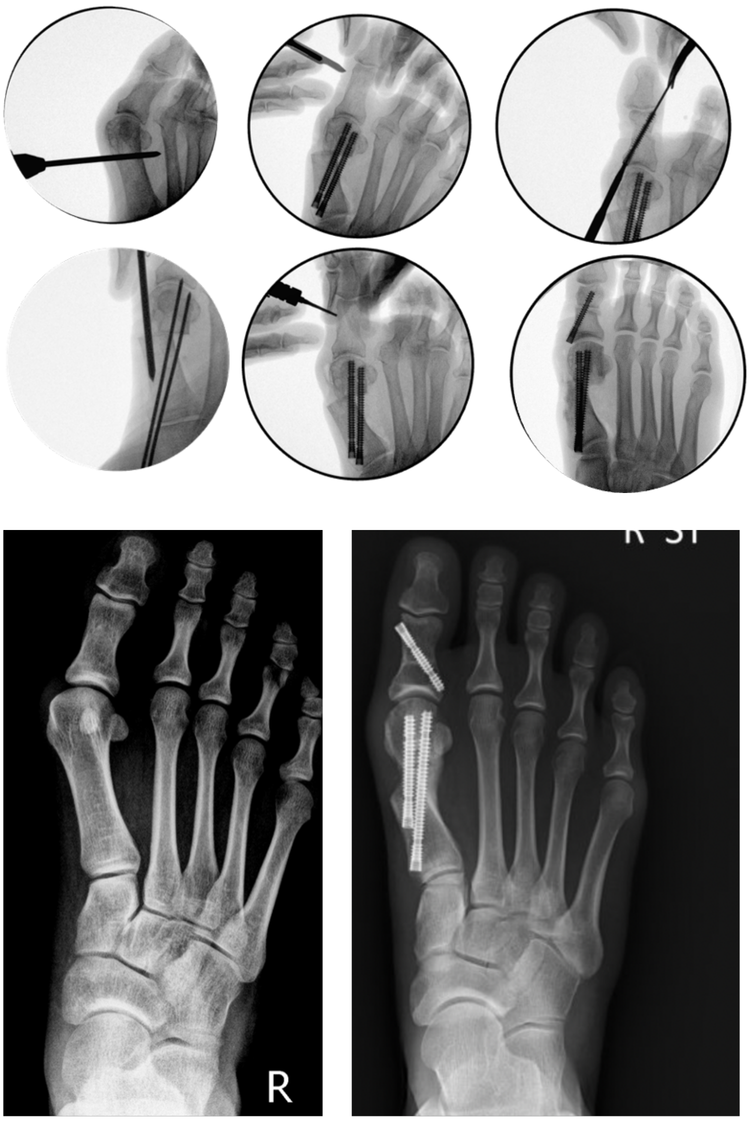

doi:10.6342/NTU202501861

Figure 6: Manual Adjustment of Plantar Zones Using the RS-Scan System

The plantar zones of the foot were manually refined after the initial automated division by the RS-Scan system. Pedobarographic data were recorded for the following regions: hallux (H), lesser toes (T2-5), first metatarsal (M1), central metatarsals (CMT, encompassing the second to fourth metatarsals), and the fifth metatarsal (M5).

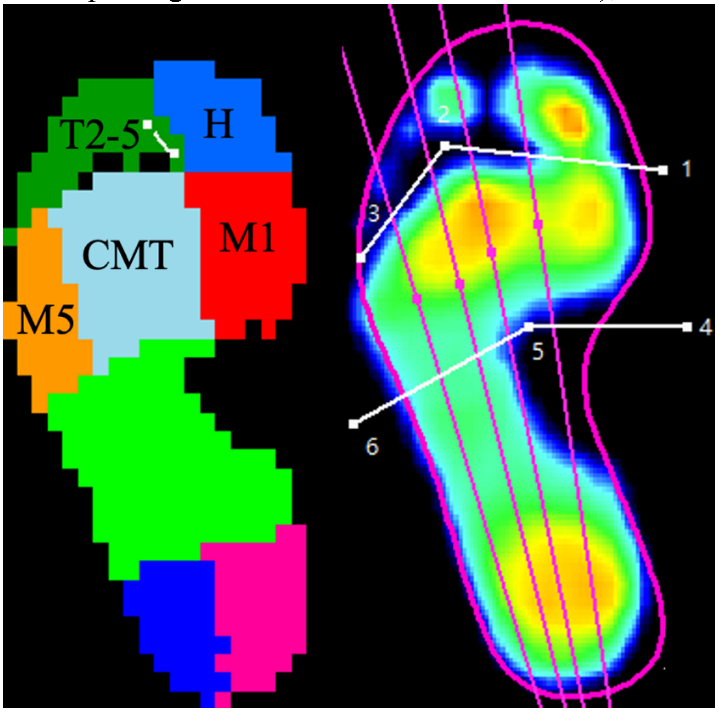

doi:10.6342/NTU202501861

Figure 7: Illustration of the study design of study 3.

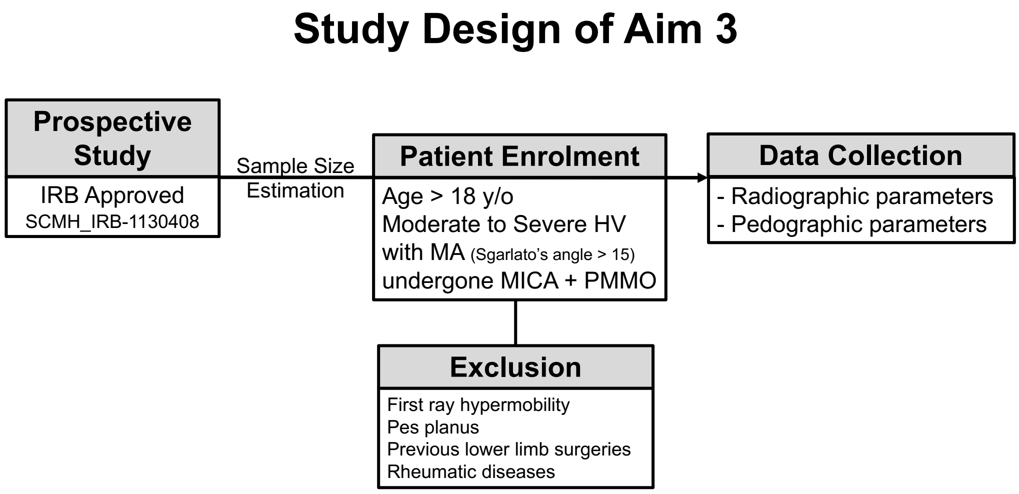

doi:10.6342/NTU202501861

Figure 8: Proximal Metatarsal Minimally invasive Osteotomy（PMMO）.

The upper pictures indicate the intraoperative radiographs of MICA and PMMO.
The lower radiographs showed a patient with hallux valgus and metatarsus adductus receiving MICA and PMMO before (left), immediately after (middle), and six months after (right) the surgery.

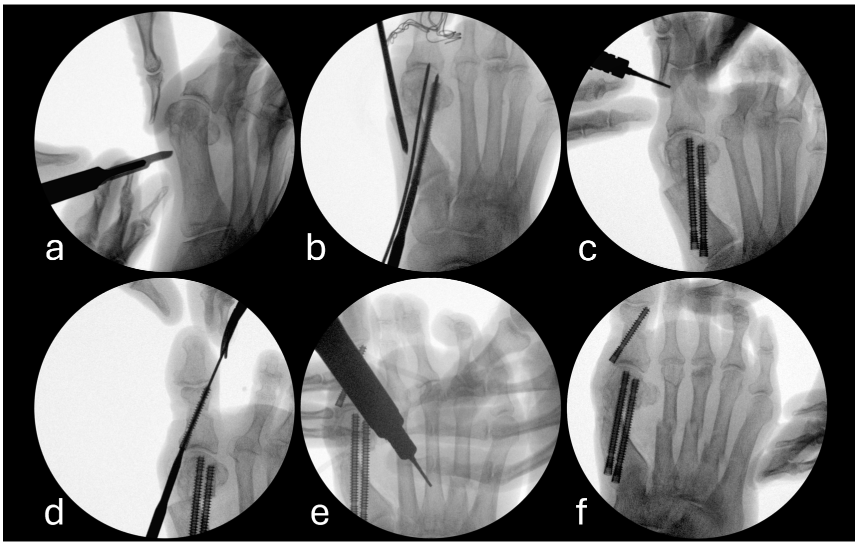

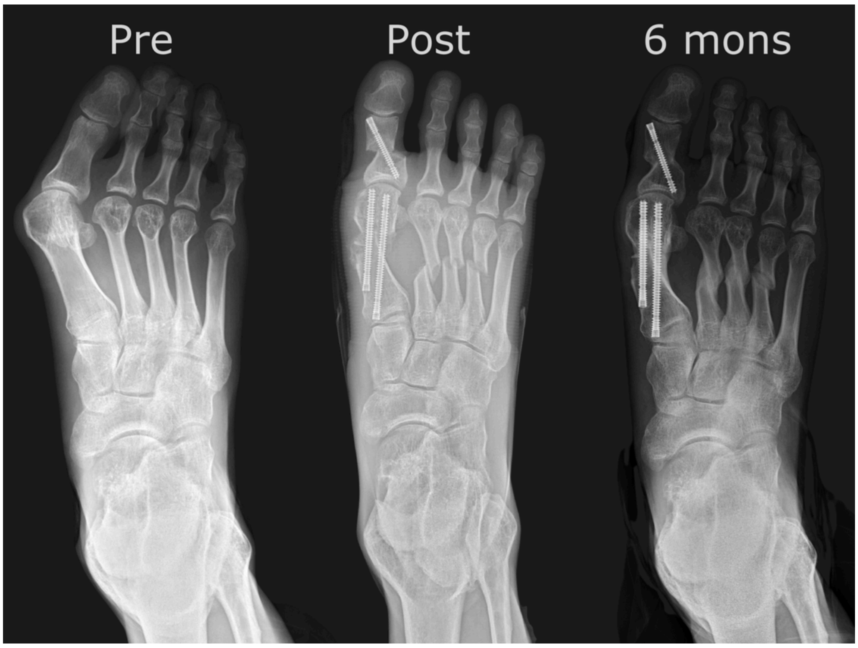

doi:10.6342/NTU202501861

TABLES

Table 1: Description of radiographic measurements relevant to pes planus in aim 1

Measurement	Descripition
Measure from a weight-bearing antero-posterior (AP) foot radiograph.	
Talonavicular coverage angle	The angle formed between a line connecting the edges of the articular surface of the talus and the articular surface of the navicular
Antero-posterior talar–1st metatarsal angle	The angle formed from a line through the mid-axis of the talus and the long axis of the 1st metatarsal
Antero-posterior talocalcaneal angle (Kite's angle)	The angle formed by a line bisecting the head and neck of the talus and a line along the lateral border of the calcaneus
Measure from a weight-bearing antero-posterior (AP) ankle mortise radiograph.	
fibular axis calcaneal offset (FACO)	The widest horizontal distance between the mid-fibular axis and the calcaneal wall just inferior to the peroneal tubercle.
Measure from a weight-bearing lateral foot radiograph.	
Lateral talar–1st metatarsal angle (Meary's angle)	The angle formed from the bisection of the long axis of the talus and the 1st metatarsal
Calcaneal inclination	The angle formed between a line from the plantar surface of the calcaneus to the inferior distal articular surface and the transverse plan
Lateral talocalcaneal angle	The angle formed between a line bisecting the talus and a line from the plantar surface of the calcaneus to the inferior distal articular surface
Moreau-Costa-Bartani angle	The angle formed between a line from the inferior posterior calcaneal tuberosity to the inferior border of the talonavicular joint and a line from the medial sesamoid to the inferior border of the talonavicular joint
Talar declination	The angle formed between a line drawn along the long axis of the talus and the transverse plane

doi:10.6342/NTU202501861

Table 2: Univariate logistic regression determined odds ratios for predicting AOFAS and FAOS scores.

Preoperative										
		Talonavicular coverage angle	Antero-posterior talar－1st metatarsal angle	Antero-posterior talocalcaneal angle	FACO	Meary's angle	Talar declination	Calcaneal inclination	Lateral talocalcaneal angle	Moreau-Costa-Bartani angle
AOFAS	Odds ratio	-0.6954	0.1478	-0.394	0.08212	-0.6506	-0.4026	0.3534	-0.3799	-0.1645
	p value	< 0.01	0.2615	0.02	0.6662	< 0.01	0.01	0.03	0.02	0.33
FAOS	Odds ratio	-0.4986	-0.2462	0.003101	0.05539	-0.4865	-0.4402	0.2606	-0.4446	0.0302
	p value	< 0.01	0.1478	-0.4672	0.7713	< 0.01	< 0.01	0.1248	< 0.01	0.8612
Postoperative										
AOFAS	Odds ratio	-0.6478	0.1045	-0.295	0.05355	-0.5112	-0.4918	-0.09368	-0.3054	-0.1362
	p value	< 0.01	0.5324	0.07214	0.7495	< 0.01	< 0.01	0.5759	0.06226	0.4148
FAOS	Odds ratio	-0.5042	0.009472	-0.468	-0.06207	-0.5782	-0.6324	-0.05581	-0.3641	-0.1691
	p value	< 0.01	0.955	< 0.01	0.7112	< 0.01	< 0.01	0.7393	0.02	0.3101

AOFAS, American Orthopedic Foot and Ankle Score; FAOS, Foot and Ankle Outcome Score; FACO, fibular axis calcaneal offset

doi:10.6342/NTU202501861

Table 3: Cut-off Values from ROC Analysis for Key Angles

	Cut-off value	AOFAS score	FAOS score
Talonavicular coverage angle	28.5 degrees	AUC: 0.74 Sensitivity: 55% Specificity: 92.5%	AUC: 0.9 Sensitivity: 83.3% Specificity: 90%
Meary's angle	19.5 degrees	AUC: 0.69 Sensitivity: 50% Specificity: 88.5%	AUC: 0.93 Sensitivity: 83.3% Specificity: 83.3%
Talar declination	37.5 degrees	AUC: 0.69 Sensitivity: 50% Specificity: 82.15%	AUC: 0.77 Sensitivity: 67% Specificity: 82.8%

AOFAS, American Orthopedic Foot and Ankle Score; FAOS, Foot and Ankle Outcome Score; AUC, area under the receiver operating characteristic curve

doi:10.6342/NTU202501861

Table 4: Demographics of study population of aim 2. (n = 31 feet).

Demographics	Average ± Standard Deviation
Age (years old)	50.83 ± 12.38
Height (cm)	156.84 ± 3.07
Weight (kg)	53.38 ± 9.21
BMI (kg/cm^2)	21.69 ± 3.40

BMI—body mass index.

doi:10.6342/NTU202501861

Table 5: Perioperative radiographic changes of aim 2

	Pre-Op	Post-Op 3M	Change	*p* Value	Effect Size
HVA	31.90 ± 6.30 (21.27–46.59)	7.97871 ± 6.11 (0.48–17.46)	−23.92 ± 6.52	<0.001 *	3.85
IMA	14.2016 ± 2.61 (12.25–18.65)	5.94871 ± 3.20 (1.23–10.04)	−8.25 ± 2.74	<0.001 *	2.83
DMAA	30.9923 ± 9.91	9.40323 ± 7.91	−21.59 ± 7.68	<0.001 *	2.41
MT1L	65.49 ± 4.79	62.33 ± 5.63			
MT2L	77.79 ± 5.83	76.91 ± 6.81			
MT1CL	65.49 ± 4.79	63.06 ± 4.99	−2.43 ± 2.54	<0.001 *	0.50
MT2PD	11.41 ± 2.58	11.17 ± 2.43	−0.25 ± 1.68	0.422	0.10
MT1LHS	Round: 14 (45%) Intermediate: 7 (23%) Angular: 10 (32%)	Round: 6 (19%) Intermediate: 11 (35%) Angular: 14 (45%)		<0.001 #	
LSG	Normal: 0 (0%) Mild: 5 (16%) Moderate: 15 (48%) Severe: 11 (35%)	Normal: 3 (10%) Mild: 16 (52%) Moderate: 9 (29%) Severe: 3 (10%)		<0.001 #	
LMA	7.397 ± 7.46	6.58 ± 6.59	−0.81 ± 5.83	0.443 *	0.12
CPA	19.55 ± 5.22	19.58 ± 4.45	0.035 ± 2.73	0.942 *	0.01

Data are expressed as mean ± standard deviation (range) or counts and percentages. HVA—hallux valgus angle; IMA—intermetatarsal angle; DMAA—distal metatarsal articular angle; MT1L—1st metatarsal length; MT2L—2nd metatarsal length; MT1CL—corrected 1st metatarsal length; MT2PD—2nd metatarsal protrusion distance; MT1LHS—1st metatarsal lateral head shape; LSG—lateral sesamoid grade; LMA—lateral Meary's angle; CPA—calcaneal pitch angle. * p value < 0.05 was considered statistically significant using the two-tailed t-test. # p value < 0.05 was considered statistically significant using the two-sided Wilcoxon signed-rank test. Effect size was calculated using Cohen's d.

doi:10.6342/NTU202501861

Table 6: Perioperative maximal plantar force (N) change in different plantar areas in aim 2.

	Pre-Op	Post-Op 3M	Change	*p* Value	Effect Size
Hallux	44.59 ± 21.61	23.56 ± 12.79	−21.04 ± 24.43	<0.001 *	1.18
Toe 2–5	26.12 ± 15.78	27.85 ± 12.98	+1.72 ± 14.92	0.525	0.12
M1	69.06 ± 29.97	52.73 ± 13.90	−16.34 ± 28.14	0.003 *	0.70
M2–4	251.98 ± 58.18	251.08 ± 51.55	−0.90 ± 59.50	0.934	0.02
M5	40.49 ± 15.66	43.99 ± 19.02	+3.50 ± 16.95	0.260	0.20

Data are expressed as mean ± standard deviation. M1—first metatarsal; M2–4—second to fourth metatarsals; M5—fifth metatarsal. * p value < 0.05 was considered statistically significant using the two-tailed t test. Effect size was calculated using Cohen's d.

doi:10.6342/NTU202501861

Table 7: Perioperative maximal plantar pressure (kPa) changes in different plantar areas in aim 2

	Pre-Op	**Post-Op 3M**	**Change**	***p* Value**	**Effect Size**
Hallux	33.30 ± 14.70	20.00 ± 11.23	−13.30 ± 17.46	<0.001 *	1.02
Toe 2–5	16.62 ± 11.77	15.44 ± 7.92	−1.18 ± 10.60	0.539	0.12
M1	43.12 ± 17.84	35.32 ± 9.89	−7.80 ± 18.78	0.028 *	0.54
M2–4	81.18 ± 18.64	81.03 ± 17.28	−0.15 ± 22.10	0.970	0.01
M5	33.98 ± 11.69	37.72 ± 14.81	+3.74 ± 14.81	0.170	0.28

Data are expressed as mean ± standard deviation. M1—first metatarsal; M2–4—second to fourth metatarsals; M5—fifth metatarsal. * p value < 0.05 was considered statistically significant using the two-tailed t test. Effect size was calculated using Cohen's d.

doi:10.6342/NTU202501861

Table 8: Perioperative force–time integral (Ns) changes in different plantar areas in aim 2

	Pre-Op	Post-Op 3M	Change	*p* Value	Effect Size
Hallux	14.84 ± 7.32	5.21 ± 3.38	−9.63 ± 7.42	<0.001 *	1.69
Toe 2–5	7.71 ± 4.22	8.14 ± 4.04	+0.43 ± 4.39	0.584	0.10
M1	28.85 ± 10.84	20.66 ± 5.80	−8.19 ± 9.24	0.008 *	0.94
M2–4	115.55 ± 35.71	106.78 ± 30.54	−8.77 ± 23.28	0.129	0.26
M5	17.95 ± 8.01	17.41 ± 7.53	−0.55 ± 6.93	0.676	0.07

Data are expressed as mean ± standard deviation. M1—first metatarsal; M2–4—second to fourth metatarsals; M5—fifth metatarsal. * p value < 0.05 was considered statistically significant using the two-tailed t test. Effect size was calculated using Cohen's d.

doi:10.6342/NTU202501861

Table 9: Perioperative pressure–time integral (kPa s) changes in different plantar areas in aim 2

	Pre-Op	Post-Op 3M	Change	*p* Value	Effect Size
Hallux	10.82 ± 5.36	4.29 ± 2.92	−6.53 ± 5.59	<0.001 *	1.51
Toe 2–5	4.82 ± 3.23	4.32± 2.21	−0.49 ± 3.01	0.360	0.18
M1	17.99 ± 5.06	13.63 ± 3.70	−4.35 ± 5.16	0.038 *	0.98
M2–4	37.41 ± 11.08	34.25 ± 8.29	−3.16 ± 9.37	0.150	0.32
M5	15.13 ± 5.66	14.72 ± 5.13	−0.41 ± 5.68	0.712	0.08

Data are expressed as mean ± standard deviation. M1—first metatarsal; M2–4—second to fourth metatarsals; M5—fifth metatarsal. * p value < 0.05 was considered statistically significant using the two-tailed t-test. Effect size was calculated using Cohen's d.

doi:10.6342/NTU202501861

Table 10: Demographic data in aim 3.

Demographic	Average ± Standard Deviation
Numbers	25
Age (y/o)	50.1±20.8
M/F	9/16
Op time (mins)	47.2±10.0
Hospital stay (days)	3.6±0.7
Union time (days)	189.2±80.2
Height (cm)	159.3±9.6
Weight (Kg)	58.8±7.5
BMI	23.2±2.6

doi:10.6342/NTU202501861

Table 11: Perioperative radiographic changes in aim 3.

HVA-hallux valgus angle; IMA-intermetatarsal angle. ; MA(4MT)- metatarsus adductus angle Unit: degree . * statistic significant pre op vs post op 1 month, ** statistic significant pre op vs post op 6 months.

	pre op	post op 1 months	post op 6 months
HVA	44.6±10.2	6.1±7.3*	10.6±8.6**
IMA	15.6±3.3	7.2±2.6*	8.6±3.1**
MA(4MT)	16.3±4.8	7.1±4.5*	9.2±4.1**
MA(5MT)	22.1±6.1	11.9±5.8*	15.4±5.3**

doi:10.6342/NTU202501861

Table 12: Bone length before and after 6 months of surgery in aim 3.

p1-proximal phalanx of hallux; M1-first metatarsal; M2-second metatarsal; M3-third metatarsal; M4-fourth metatarsal. * p value < 0.05.

	pre op	post op	Length difference	p-value
P1	28.3±3.1	25.6±2.3	2.7±1.7	0.043*
M1	65±6.6	59.6±6.1	5.4±3.7	0.073
M2	74.1±9.3	67.0±5.3	7.1±7.2	0.050*
M3	70.4±8.2	63.1±4.5	7.3±5.9	0.023*
M4	67.8±6.9	61.9±4.3	5.8±4.5	0.035*

doi:10.6342/NTU202501861

Table 13: Perioperative maximal force (N) changes in different plantar areas in aim 3. T1-hallux; T2-5-second to fifth toes; M1-first metatarsal; M2-4-second to fourth metatarsals; M5-fifth metatarsal. * p value < 0.05.

	Pre op	**Post op**	**p-value**
T1	14.9±8.6	9.5±5.1	0.004*
T2-5	8.7±4.1	6.5±1.9	0.027*
M1	24.0±16.0	30.3±13.8	0.187
M2-4	78.6±18.0	46.5±12.9	<0.001*
M5	20.7±9.9	26.4±7.4	0.033*

doi:10.6342/NTU202501861

Table 14: Perioperative peak pressure (kPa) changes in different plantar areasin aim 3. T1-hallux; T2-5-second to fifth toes; M1-first metatarsal; M2-4-second to fourth metatarsals; M5-fifth metatarsal. * p value < 0.05.

	Pre op	Post op	p-value
T1	99.6±57.5	63.2±34.0	0.004*
T2-5	58.3±27.1	43.5±12.9	0.025*
M1	160.2±106.9	202.2±91.9	0.186
M2-4	523.9±120.1	310.1±86.0	<0.001*
M5	138.4±66.2	175.9±49.0	0.034*

doi:10.6342/NTU202501861

Table 15: Perioperative force–time integral (Ns) changes in different plantar areas in aim 3.

T1-hallux; T2-5-second to fifth toes; M1-first metatarsal; M2-4-second to fourth metatarsals; M5-fifth metatarsal. * p value < 0.05.

	Pre op	**Post op**	**p-value**
T1	4.4±4.5	1.9±1.4	0.009*
T2-5	2.3±1.5	1.4±0.9	0.007*
M1	8.1±5.7	10.0±6.1	0.340
M2-4	28.2±6.9	16.6±7.6	<0.001*
M5	7.9±3.0	9.4±2.1	0.059

doi:10.6342/NTU202501861

Table 16: Perioperative pressure–time integral (kPa·s) changes in different plantar in aim 3.

T1-hallux; T2-5-second to fifth toes; M1-first metatarsal; M2-4-second to fourth metatarsals; M5-fifth metatarsal. * p value < 0.051.

	Pre op	**Post op**	**p-value**
T1	29.1±29.9	13.1±9.5	0.010*
T2-5	15.2±10.0	9.0±5.9	0.006*
M1	53.8±37.9	66.8±40.6	0.336
M2-4	187.8±46.3	110.6±50.7	<0.001*
M5	52.5±20.2	62.4±14.1	0.063

doi:10.6342/NTU202501861

APPENDIX

Appendix 1: IRB Certificate for Aim 1.

秀傳醫療社團法人秀傳紀念醫院
Show Chwan Memorial Hospital

人體試驗委員會
Institutional Review Board

No. 542, Sec. 1, Chung-Shan Rd. Changhua, Taiwan 500, R.O.C.
Contact person: Shu-Feng Ni
Tel:886-4-7256166 ext85610 Fax:886-4-7229627
E-mail: irb@show.org.tw

500 彰化市中山路一段 542 號
聯絡人：倪淑鳳
電話：(04)7256166 #85610 傳真：(04)7229627
電子信箱：irb@show.org.tw

同意臨床試驗證明書

查檢送 骨科部 陳彥宇/朱家宏 主持『距下關節置換術用於治療兒童扁平足：長期追蹤研究』案（本會編號：1110703），經秀傳醫療社團法人秀傳紀念醫院人體試驗委員會於民國 111 年 08 月 15 日審查通過。有效期限至民國 112 年 08 月 14 日止。本會並保留監督該項研究的權利。嚴重不良事件通報、後續追蹤審查之程序及應注意事項，請參閱背面。

人體試驗委員會
主任委員
李佩淵

中 華 民 國 一 一 一 年 八 月 十 五 日

Certificate of Approval

August 15 2022

The following documents have been submitted for review.

Protocol Title: Subtalar arthroereisis for the treatment of symptomatic flexible flatfoot in pediatrics: a long-term follow-up study
Protocol Number: SRD-111008
Protocol Version: 一，2022.03.21
Informed Consent Form : 一，2022/07/30
Principle Investigator: Yan-Yu Chen
Co-Investigators: Chia-Hung Chu
SCMH_IRB No: 1110703

Above study is approved by the Institutional Review Board of Show Chwan Memorial Hospital on August 15, 2022 and valid till August 14, 2023. The Institutional Review Board of Show Chwan Memorial Hospital reserves the right to monitor the study.
See the reverse of this form for the procedures for reporting serious adverse events and for periodic follow-up, and for other important notes.

秀傳醫療社團法人秀傳紀念醫院 人體試驗委員會 Institutional Review Board 彰化市中山路一段542號

Your sincerely,
Pei-Yuan Lee
Chairman
Institutional Review Board
Show Chwan Memorial Hospital
Taiwan, R.O.C.

本會組織與執行皆遵 ICH-GCP
The Institutional Review Board performs its functions according to written operating procedures and complies with GCP and with the applicable regulatory requirements.

doi:10.6342/NTU202501861

Appendix 2: IRB Certificate for Aim 2.

秀傳醫療社團法人秀傳紀念醫院
Show Chwan Memorial Hospital

人體試驗委員會
Institutional Review Board

No. 542, Sec. 1, Chung-Shan Rd. Changhua, Taiwan 500, R.O.C.
Contact person: Shu-Feng Ni
Tel:886-4-7256166 ext88925 Fax:886-4-7229627
E-mail: irb@show.org.tw

500 彰化市中山路一段 542 號
聯絡人：倪淑鳳
電話：(04)7256166 #88925 傳真：(04)7229627
電子信箱：irb@show.org.tw

同意臨床試驗證明書

查檢送 骨科部 陳彥宇 主持『微創截骨術應用在拇趾外翻病人的足壓及影像分析』案（本會編號：1130409），經秀傳醫療社團法人秀傳紀念醫院人體試驗委員會於民國 113 年 05 月 16 日審查通過。有效期限至民國 114 年 05 月 15 日止。本會並保留監督該項研究的權利。嚴重不良事件通報、後續追蹤審查之程序及應注意事項，請參閱背面。

人體試驗委員會
主任委員
李佩淵

中 華 民 國 一 一 三 年 五 月 十 六 日

Certificate of Approval

May 16, 2024

The following documents have been submitted for review.

Protocol Title: Pedographic and Radiographic Changes after Minimally Invasive Chevron Akin osteotomy in Hallux Valgus patients
Protocol Version: V1，2024-04-25
Informed Consent Form : waive
Principle Investigator: Yan-Yu Chen
SCMH_IRB No: 1130409

Above study is approved by the Institutional Review Board of Show Chwan Memorial Hospital on May 16, 2024 and valid till May 15, 2025. The Institutional Review Board of Show Chwan Memorial Hospital reserves the right to monitor the study.
See the reverse of this form for the procedures for reporting serious adverse events and for periodic follow-up, and for other important notes.

秀傳醫療社團法人秀傳紀念醫院
人體試驗委員會
Institutional Review Board
彰化市中山路一段542號

Your sincerely,
Pei-Yuan Lee
Chairman
Institutional Review Board
Show Chwan Memorial Hospital
Taiwan, R.O.C.

本會組織與執行皆遵 ICH-GCP
The Institutional Review Board performs its functions according to written operating procedures and complies with GCP and with the applicable regulatory requirements.

doi:10.6342/NTU202501861

Appendix 3: IRB certificate for Aim3

秀傳醫療社團法人秀傳紀念醫院
Show Chwan Memorial Hospital

人體試驗委員會
Institutional Review Board

No. 542, Sec. 1, Chung-Shan Rd. Changhua, Taiwan 500, R.O.C.
Contact person: Shu-Feng Ni
Tel:886-4-7256166 ext88925 Fax:886-4-7229627
E-mail: irb@show.org.tw

500 彰化市中山路一段 542 號
聯絡人：倪淑鳳
電話：(04)7256166 #88925 傳真：(04)7229627
電子信箱：irb@show.org.tw

同意臨床試驗證明書

查檢送 骨科部 陳彥宇/黃俊憲 主持『微創截骨術應用在拇趾外翻合併蹠骨內翻病人的足壓及影像分析』案（本會編號：1130408），經秀傳醫療社團法人秀傳紀念醫院人體試驗委員會於民國 113 年 06 月 04 日審查通過。有效期限至民國 114 年 06 月 03 日止。本會並保留監督該項研究的權利。嚴重不良事件通報、後續追蹤審查之程序及應注意事項，請參閱背面。

人體試驗委員會
主任委員
李佩淵

中 華 民 國 一 一 三 年 六 月 四 日

Certificate of Approval

June 4, 2024

The following documents have been submitted for review.

Protocol Title: Pedograph and radiologh analysis in patient with hallux valgus and metatarsus adductus who received minimally invasive chevron akin procedure supplemented by proximal minimally invasive metatarsal osteotomy.

Protocol Version: V1.2，2024-5-7

Informed Consent Form : waive

Principle Investigator: Yan-Yu Chen

Co-Investigators: Chun-Hsien Huang

SCMH_IRB No: 1130408

Above study is approved by the Institutional Review Board of Show Chwan Memorial Hospital on June 4, 2024 and valid till June 3, 2025. The Institutional Review Board of Show Chwan Memorial Hospital reserves the right to monitor the study.
See the reverse of this form for the procedures for reporting serious adverse events and for periodic follow-up, and for other important notes.

秀傳醫療社團法人秀傳紀念醫院 人體試驗委員會 Institutional Review Board 彰化市中山路一段542號

Your sincerely,
Pei-Yuan Lee
Chairman
Institutional Review Board
Show Chwan Memorial Hospital
Taiwan, R.O.C.

本會組織與執行皆遵 ICH-GCP
The Institutional Review Board performs its functions according to written operating procedures and complies with GCP and with the applicable regulatory requirements.

doi:10.6342/NTU202501861